The Saccharomyces cerevisiae quinone oxidoreductase Lot6p: stability, inhibition and cooperativity

Megarity, C. F., Looi, H. K., & Timson, D. J. (2014). The Saccharomyces cerevisiae quinone oxidoreductase Lot6p: stability, inhibition and cooperativity. *FEMS Yeast Research*, *14*(5), 797-807. https://doi.org/10.1111/1567-1364.12167

Published in:
FEMS Yeast Research

Document Version:
Early version, also known as pre-print

Queen's University Belfast - Research Portal:
Link to publication record in Queen's University Belfast Research Portal

Publisher rights
This is the pre-peer reviewed version of the following article: Megarity, C. F., Looi, H. K. and Timson, D. J. (2014), The Saccharomyces cerevisiae quinone oxidoreductase Lot6p: stability, inhibition and cooperativity. FEMS Yeast Research, 14: 797–807. doi: 10.1111/1567-1364.12167, which has been published in final form at http://onlinelibrary.wiley.com/doi/10.1111/1567-1364.12167/abstract;jsessionid=F6B9B9C09D620717AC66793D6E6E4EC5.f03t01

General rights
Copyright for the publications made accessible via the Queen's University Belfast Research Portal is retained by the author(s) and / or other copyright owners and it is a condition of accessing these publications that users recognise and abide by the legal requirements associated with these rights.

Take down policy
The Research Portal is Queen's institutional repository that provides access to Queen's research output. Every effort has been made to ensure that content in the Research Portal does not infringe any person's rights, or applicable UK laws. If you discover content in the Research Portal that you believe breaches copyright or violates any law, please contact openaccess@qub.ac.uk.

Download date:05. May. 2023

FEMS YEAST RESEARCH

http://mc.manuscriptcentral.com/fems

The Saccharomyces cerevisiae quinone oxidoreductase Lot6p: stability, inhibition and cooperativity

Journal:	*FEMS Yeast Research*
Manuscript ID:	Draft
Manuscript Type:	Research Paper
Date Submitted by the Author:	n/a
Complete List of Authors:	Megarity, Clare; Queen's University, Belfast, School of Biological Sciences Looi, Hong Keat; Queen's University, Belfast, School of Biological Sciences Timson, David; Queen's University, Belfast, School of Biological Sciences
Keywords:	Quinone oxidoreductase, resveratrol, negative cooperativity, nitroreductase, FMN-containing enzyme
Note: The following files were submitted by the author for peer review, but cannot be converted to PDF. You must view these files (e.g. movies) online.	
Lot6p_curcumin.pdb Lot6p_nicotinamide.pdb Lot6p_resveratrol.pdb	

SCHOLARONE™
Manuscripts

Dr David J Timson
Reader in Biochemistry
School of Biological Sciences
Queen's University, Belfast
Medical Biology Centre
97 Lisburn Road
BELFAST
BT9 7BL
Tel: (028) 9097 5875
Email: d.timson@qub.ac.uk

Prof J Nielsen
Chief Editor - FEMS Yeast Research
Department of Chemical and Biological Engineering
Chalmers University of Biotechnology
GOTHENBURG
Sweden

13th February 2013

Dear Prof Nielsen

We would like you to consider our paper entitled "The *Saccharomyces cerevisiae* quinone oxidoreductase Lot6p: inhibition, stability and cooperativity" for publication in FEMS Yeast Research.

We believe that this paper is suitable for publication because:

1. It documents the steady state enzyme kinetics of Lot6p with NADH as well as with NADPH (which has been the focus of previous studies).
2. It establishes assays to measure the thermal stability of Lot6p and shows that several compounds can stabilize Lot6p in a concentration dependent manner.
3. It shows that the same group of compounds act as inhibitors of Lot6p – and that some of these compounds act with negative cooperativity, inferring information transmission is possible between the active sites. To our knowledge, this is the first report of negative cooperativity in Lot6p (or the functionally related "nitroreductase" enzymes in bacteria).
4. It presents molecular models which suggest a plausible molecular mechanism for this information transmission.
5. It presents an experimental test of this mechanism by altering a key residue in the proposed communication pathway which reduces the degree of cooperativity observed.

We hope that you will agree that this paper is suitable for publication and look forward to hearing from you in the near future.

Yours sincerely

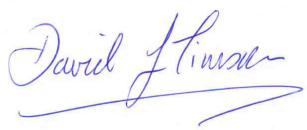

David J Timson

For Peer Review

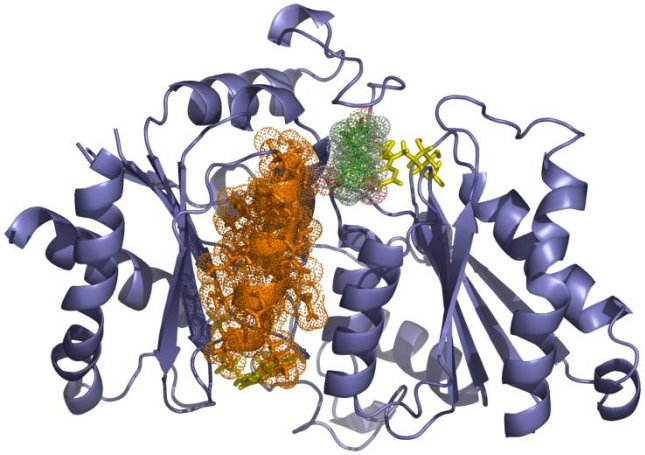

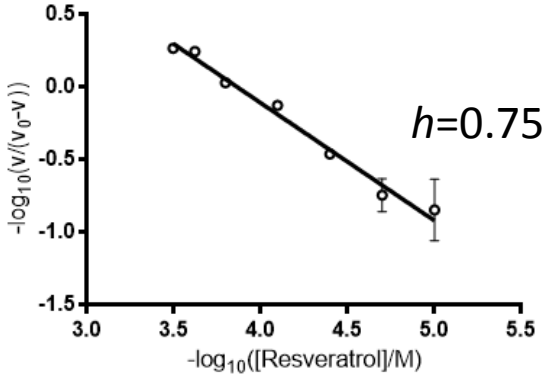
0.5
0.0
-0.5
-1.0
-1.5
3.0
3.5
4.0
4.5
5.0
5.5
-log10(v/(v0-v))
-log10([Resveratrol]/M)
h=0.75

The *Saccharomyces cerevisiae* quinone oxidoreductase Lot6p: stability, inhibition and cooperativity

Clare F. Megarity, Hong Keat Looi & David J. Timson*

School of Biological Sciences, Queen's University Belfast, Medical Biology Centre, 97 Lisburn Road, Belfast, BT9 7BL. UK.

*Author to whom correspondence should be addressed.

Telephone +44(0)28 9097 5875

Fax +44(0)28 9097 5877

Email d.timson@qub.ac.uk

Running title: Lot6p: stability, inhibition and cooperativity

For Peer Review

ScholarOne Support 1-434/964-4100

Abstract

Lot6p (EC 1.5.1.39; Ylr011wp) is the sole quinone oxidoreductase in the budding yeast, *Saccharomyces cerevisiae*. Using hexahistdine tagged recombinant Lot6p, we demonstrated that the enzyme can function with either NADH or NADPH as an electron donor; no cooperativity was observed with these substrates. The NQO1 inhibitor curcumin, the NQO2 inhibitor resveratrol, the bacterial nitroreductase inhibitor nicotinamide and the phosphate mimic vanadate all stabilise the enzyme as judged by thermal scanning fluorimetry. All except vanadate have no observable effect on the chemical crosslinking of the two subunits of the Lot6p dimer. These compounds all inhibit Lot6p's oxidoreductase activity and all except nicotinamide exhibit negative cooperativity. Molecular modelling suggests that curcumin, resveratrol and nicotinamide all bind over the isoalloxazine ring of the FMN cofactor in Lot6p. However, resveratrol and curcumin stretch further from the cofactor and contact an α-helix that links the two active sites. Mutation of Gly-142, which forms part of this helix, to serine does not greatly affect the kinetics or stability of the enzyme. However, this variant shows less cooperativity towards resveratrol and vanadate. This suggests a plausible hypothesis for the transmission of information between the subunits and, thus, the molecular mechanism of negative cooperativity in Lot6p.

Keywords: Quinone oxidoreductase; resveratrol; negative cooperativity; nitroreductase; FMN-containing enzyme

For Peer Review

ScholarOne Support 1-434/964-4100

Introduction

Many species contain relatively non-specific quinone oxidoreductases. The best characterised of these is the human NAD(P)H quinone oxidoreductase 1 (NQO1, DT-diaphorase, EC 1.6.5.2). This enzyme has attracted considerable interest because of its role in vitamin K metabolism, its potential as an anti-cancer drug target and its ability to stabilise the tumour suppressor protein p53 (Anwar *et al.*, 2003; Gong *et al.*, 2007; Nolan *et al.*, 2007; Gong *et al.*, 2008; Dinkova-Kostova & Talalay, 2010; Tie *et al.*, 2011). NQO1 is a dimeric enzyme with an FAD cofactor tightly bound to both subunits (Li *et al.*, 1995). This enzyme is a target for the anticoagulant drug dicoumarol (Hosoda *et al.*, 1974; Rase *et al.*, 1976). In humans, there is a second, structurally similar enzyme, NQO2 (EC 1.10.99.2) (Long & Jaiswal, 2000; Vella *et al.*, 2005). The functions and substrates of NQO2 are currently less clear, although it is known that this enzyme is inhibited by resveratrol (Buryanovskyy *et al.*, 2004). Bacteria have a range of quinone oxidoreductases including the NQO1-like MdaB, the tetrameric oxidoreductase WrbA, the azoreductase AzoR and the so-called nitroreductases (e.g. NemA, NfsA, NfsB, YdjA) (Zenno *et al.*, 1996a; Zenno *et al.*, 1996b; Kobori *et al.*, 2001; Lovering *et al.*, 2001; Adams & Jia, 2006; Ito *et al.*, 2006; Patridge & Ferry, 2006; Andrade *et al.*, 2007; Carey *et al.*, 2007; Choi *et al.*, 2008; Hong *et al.*, 2008; Prosser *et al.*, 2010; Mercier *et al.*, 2013). The name of the last group arises due to their ability to catalyse the reduction of a range of nitrogenous compounds, for example nitrobenzene, trinitrotoluene, chloramphenicol, and the pro-drug 5-(aziridin-1-yl)-2,4-dinitrobenzamide (CB1954) (Anlezark *et al.*, 1992; Caballero *et al.*, 2005; Smith *et al.*, 2007; Yanto *et al.*, 2010). In the budding yeast, *Saccharomyces cerevisiae*, there is one such enzyme, Lot6p (EC 1.5.1.39; Ylr011wp) (Zhang *et al.*, 2001). This enzyme resembles the bacterial azo- and nitroreductases in

For Peer Review

that it is dimeric and uses FMN, not FAD, as its tightly bound cofactor (Liger *et al.*, 2004). Despite this difference it still catalyses similar reactions to NQO1 and MdaB (Liger *et al.*, 2004; Sollner *et al.*, 2007).

All quinone oxidoreductases characterised to date have a substituted enzyme ("ping-pong") mechanism in which a reducing agent (usually NADH or NADPH), transfers a hydride to the FAD or FMN cofactor. The oxidised $NAD(P)^+$ then leaves the active site, enabling the second substrate to enter and be reduced by the cofactor (Hosoda *et al.*, 1974; Sollner *et al.*, 2007; Sollner *et al.*, 2009b). The range of possible substrates is broad. In addition to a wide range of quinones and quinone derivatives, human NQO1 has been shown *in vitro* to catalyse the reduction of aromatic nitrogen compounds and iron(III) ions (Sarlauskas *et al.*, 1997; Anusevicius *et al.*, 2002; Miseviciene *et al.*, 2006; Newsome *et al.*, 2007; Onyenwoke & Wiegel, 2007).

Lot6p was first identified as the protein encoded by one of a diverse group of low temperature (*LOT*) sensitive genes. This group also included fructose 1,6-*bis*phosphate aldolase (*FBA1* or *LOT1*), a ribosomal subunit (*RPL2B* or *LOT2*), a nucleolar RNA processing enzyme (*NOP1* or *LOT3*), a gene of unknown function (*LOT5*) (Zhang *et al.*, 2001). The structure of Lot6p has been solved and revealed a typical flavodoxin fold (Liger *et al.*, 2004). The enzyme has been shown to catalyse the NADPH-dependent reduction of a range of biologically relevant quinones including 1,4-benzoquinone, 1,4-naphthoquinone and duroquinone (Sollner *et al.*, 2007) in addition to ferricyanide, azo dyes and nitrocompounds (Liger *et al.*, 2004). The activity with quinones is important in minimising toxicity by these compounds: a strain deleted for *LOT6* is less viable than the wild-type in the presence of micromolar

For Peer Review

ScholarOne Support 1-434/964-4100

concentrations of 1,4-benzoquinone, whereas one which overexpressed the protein was more viable (Sollner *et al.*, 2007). Like NQO1, Lot6p has roles beyond its enzymatic activity. It interacts directly with the 20S proteasome. Reduction of the FMN in 20S-associated Lot6p results in the recruitment of the transcription factor Yap4p and protects Yap4p from proteosomal degradation (Sollner *et al.*, 2009c). Lot6p also induces apoptosis: strains deleted for *LOT6* are less likely to undergo apoptosis when challenged with hydrogen peroxide (Sollner *et al.*, 2009a).

In contrast to mammalian NQO1 and NQO2, relatively little data has been collected on the biochemical properties of Lot6p. Here we extend previous enzymological and biochemical work by describing Lot6p's kinetics, inhibition and stability to thermal denaturation. We describe, for the first time in detail, the enzyme's kinetics with NADH as a reducing agent and quantify its inhibition by the organic compounds curcumin, resveratrol and nicotinamide. These compounds were selected for their ability to bind to the active sites of NQO1, NQO2 and bacterial nitroreductases respectively (Buryanovskyy *et al.*, 2004; Tsvetkov *et al.*, 2005; LinWu *et al.*, 2012). Vanadate ions were also studied as a phosphate analogue. In some cases, but not all, these compounds acted with negative cooperativity. Models of Lot6p in complex with these compounds were built in order to help explain their different behaviour. These models informed site-directed mutagenesis studies which further illuminated cooperativity in Lot6p.

Materials and Methods

Expression and purification of wild type and mutant Lot6p

ScholarOne Support 1-434/964-4100

For Peer Review

The coding sequence for *LOT6* was amplified by PCR using a single colony from *Saccharomyces cerevisiae* strain BY4741 (MATa; his3Δ1; leu2Δ0; met15Δ0; ura3Δ0; EUROSCARF Consortium, Germany) as a template. The product was inserted into pET-46 Ek/LIC (Merck, Nottingham, UK) and competent *E. coli* cells (NovaBlue GigaSingles, Merck) were transformed with the annealed Ek/LIC vector and insert. Colonies resulting from this transformation were picked and grown shaking at 37 °C overnight in 5 ml of Luria-Burtani (LB) broth supplemented with ampicillin (100 μg ml^{-1}), plasmid DNA was isolated using a miniprep kit (Yorkshire Biosciences, York, UK) and the presence of inserts verified by restriction digestion and PCR. Competent *E. coli* HMS174(DE3) were transformed with the plasmid DNA and a single colony picked and grown shaking overnight at 37 °C in 100 ml of LB supplemented with ampicillin (100 μg ml^{-1}); DNA was isolated using a midiprep kit (Sigma, Poole, UK) and sequenced by GATC Biotech, (Konstanz, Germany).

Another colony was picked and grown overnight shaking at 37 °C in 5 ml of LB broth supplemented with 100 μgml^{-1} ampicillin. The culture was diluted into 1 l of the same medium and grown at 37 °C for 4 h until mid-log phase was reached (A_{600}~0.6). The culture was induced by the addition of IPTG to a final concentration of 1.7 mM, and grown for a further 4 h at 37 °C. The cells were then collected by centrifugation at 4200 *g* for 15 min and the pellets resuspended in buffer R (50mM HEPES-OH pH 7.4; 150mM NaCl; 10% v/v glycerol). Sonication on ice (30 s pulses at 100 W with 30 s breaks for cooling) broke the cells and insoluble material was removed by centrifugation (24,000 *g* for 15 min). The supernatant was poured into a column containing 1 ml cold nickel agarose resin (His-select, Sigma, Poole, UK) which had been pre-equilibrated with 25 ml of buffer A (50 mM HEPES-OH pH 7.4; 500 mM

ScholarOne Support 1-434/964-4100

For Peer Review

NaCl; 10% v/v glycerol), and allowed to pass through under gravity. The column was then washed with 50 ml of buffer A. Lot6p was eluted by application of two 2 ml volumes of buffer A supplemented with imidazole (250 mM). The fraction(s) containing Lot6p was identified by 10% SDS-PAGE and were dialysed overnight at 4 °C against 1 l of buffer R supplemented with 2 mM dithiothreitol (DTT).

Site-directed mutagenesis was carried out by the QuikChange method (Wang & Malcolm, 1999) and the mutation verified by DNA sequencing of the complete *LOT6* coding sequence (GATC Biotech). The mutant enzyme was expressed and purified using the same procedures as for the wild type.

Protein concentrations were determined using the method of Bradford (Bradford, 1976) using BSA as a standard and the purified Lot6p stored in 20 µl and 50 µl aliquots frozen at -80 °C.

Enzyme kinetic analysis of Lot6p

Lot6p activity was measured at 30 ºC in 50 mM HEPES, pH 7.3 using either NADH or NADPH as the electron donor and DCPIP as the electron acceptor. Reaction rates were determined by measuring the rate of decrease in absorbance at 600 nm resulting from the reduction of DCPIP (70 µM). The enzyme concentration ranged from 1.25 nM to 10 nM. Absorbance readings were taken every 5 s and all reactions were carried out in triplicate in 96-well plates. A calibration curve of A_{600} against [DCPIP] was constructed in triplicate in a 96-well plate to determine a value for εL in the Beer Lambert Law, A=εLc were A is absorbance, c is concentration, ε is the molar extinction coefficient of DCPIP and L is the pathlength. The resulting equation of the

ScholarOne Support 1-434/964-4100

For Peer Review

line was used to convert all rates in terms of change in absorbance at 600 nm, to rates in terms of change in concentration of DCPIP.

To ensure initial, enzyme-catalyzed rates were obtained, rates for the non-enzymatic, direct reduction of DCPIP by both NADH and NADPH were determined at each concentration of electron donor with 70 μM DCPIP. These background rates were then subtracted from the rates obtained from the linear section at the beginning of each progress curve with enzyme included.

$K_{m,app}$ and $V_{max,app}$ values for each electron donor were determined, at a constant DCPIP (70 μM) by plotting enzyme-catalyzed rate (v) divided by the enzyme concentration ([E]) against the corresponding NADH or NADPH concentration. The data were fitted to a modified form of the Michaelis-Menten equation (1) using non-linear curve fitting (Marquardt, 1963) as implemented in Graphpad Prism 5.0 (GraphPad Software Inc, CA, USA.). All points were weighted equally.

$$v/[E]=k_{cat,app}[S]/K_{m,app}+[S] \quad (1)$$

where $k_{cat,app}$ is the apparent turnover number (equal to the apparent maximal rate, $V_{max,app}$, divided by the enzyme concentration), $K_{m,app}$ is the apparent Michaelis-Menten constant, [E] is the concentration of Lot6p dimer and [S] is the concentration of either NADH or NADPH.

Inhibition kinetics

The effect of potential inhibitors (resveratrol, nicotinamide, curcumin and vanadate ions) on the enzyme-catalyzed rate measured at three concentrations of NADH and three concentrations of NADPH with a constant DCPIP concentration (70 μM).

ScholarOne Support 1-434/964-4100

For Peer Review

Dilution series of resveratrol and curcumin were prepared such that the final volume of DMSO in each reaction mixture was 0.5% (v/v). Nicotinamide and sodium metavanadate were dissolved in 50 mM HEPES pH 7.3. Dixon plots (Dixon, 1953) for each concentration of electron donor were constructed and the apparent inhibition constant, $K_{i,app}$ was obtained by determining the inhibitor concentration at which the lines corresponding to each NAD(P)H concentration intercepted.

A concentration range for each inhibitor was chosen based on these $K_{i,app}$ values and an inhibitor titration was carried out using a concentration approximately equal to $K_{m,app}$ for NADH (250 μM) or NADPH (100 μM) and DCPIP (70 μM). Linearized Hill plots($-\log_{10}(v/(v_0-v))$ against $-\log_{10}$[inhibitor], where v is the rate of the inhibited reaction and v_0 is the rate in the absence of inhibitor) were constructed for each inhibitor; the gradient of these is the Hill coefficient, h (Hill, 1910).

Crosslinking and limited proteolysis

Increasing concentrations of the chemical cross-linkers *bis*sulfosuccinimidylsuberate (BS^3) and *N*-(3-Dimethylaminopropyl)-*N*′-ethylcarbodiimide hydrochloride (EDC) were added to a constant concentration of Lot6p (35 μM dimer) which had been preincubated at 30 °C for 5 min. The reaction was allowed to proceed for 30 min after which time it was stopped by the addition of an equal volume of SDS loading buffer (120 mM TrisHCl pH 6.8, 4% (w/v) SDS, 20% (v/v) glycerol, 5% (w/v) bromophenol blue, 1% (w/v) DTT). Samples were denatured by heating at 95 °C for 5 min and analysed by 10% SDS PAGE. An optimum concentration of each crosslinker was chosen and the reaction repeated in the presence of each inhibitor.

For Peer Review

ScholarOne Support 1-434/964-4100

Differential scanning fluorimetry

Lot6p was diluted in 50 mM HEPES, pH 7.3 to final concentration of 0.25 µM dimer in a final volume of 20 µl. The samples were loaded, in triplicate, into a Rotor-Gene Q cycler (Qiagen) and the high resolution melt protocol was used. Lot6p was subjected to an increase in temperature from 25 °C to 95 °C in steps of 1 K (no gain optimisation) with excitation at 460 nm and emission measured at 510 nm throughout, thereby exploiting the fluorescence of its cofactor, FMN (Forneris *et al.*, 2009). The melting temperature (T_m) of the enzyme was determined from the first derivative of the melting curve, using the inbuilt analysis software. A dilution series of each ligand (except curcumin which fluoresces in the same region as FMN (Chignell *et al.*, 1994)) was prepared such that the final volume of DMSO in the reaction mixture was 0.5% v/v. Reactions were prepared in triplicate and kept on ice until loading into the instrument. The melting temperature for each concentration of ligand was plotted against the corresponding concentration of ligand and the data were fitted to equation (2) using non-linear curve fitting in GraphPad Prism.

$$\Delta T_m = \Delta T_{m,max}[\text{ligand}]/(K_{D,app}+[\text{ligand}]) \qquad (2)$$

where $\Delta T_{m\,max}$ is the maximum, limiting change in melting temperature (T_m), and $K_{D,app}$ is the apparent dissociation constant for ligand and Lot6p.

Molecular modelling

Models of Lot6p with ligands bound were based on the experimentally determined x-ray crystal structure (PDB: 1T0I) (Liger *et al.*, 2004). This structure was aligned with that of NQO2 with resveratrol bound (PDB: 1SG0 (Buryanovskyy *et al.*, 2004)) using PyMol (http://www.pymol.org). Lot6p and the resveratrol molecules were saved into a single .pdb file which was then energy minimised and computationally

ScholarOne Support 1-434/964-4100

For Peer Review

solvated using YASARA (Krieger *et al.*, 2009) to generate the final model. Nicotinamide was modelled using the structure of NQO1 bound to $NADP^+$ (Li *et al.*, 1995). In this case, the structural alignment between the proteins was poor and so the structures were aligned using three atoms (C8, N3 and N10) in the isoalloxazine ring of the FAD or FMN cofactor. $NADP^+$ was then inserted into the Lot6p structure and this was used as a template to insert a nicotimamide molecule (from the RCSB PDB Ligand Expo; http://ligand-expo.rcsb.org/) which overlapped the nicotinamide moiety of $NADP^+$. The resulting structure was then energy minimised in YASARA to create the final model. Since there are no currently available structures of curcumin bound to a quinone oxidoreductase, this molecule was fitted into the active site by aligning the O1, C9 and C14 atoms of resveratrol with equivalent atoms in one ring of curcumin (from Ligand Expo) and assuming that the molecule adopts a similar orientation in Lot6p's active site. This initial model was then energy minimised in YASARA to generate the final model. The three final models are available as supplementary data to this paper.

Results

Recombinant expression and dimerisation of Lot6p

Lot6p can be expressed in, and purified from, *E. coli* with a typical yield of approximately 12 mg purified protein per litre of initial culture (Fig 1a). Crosslinking with both EDC and BS^3 showed that Lot6p is a dimer (Fig. 1b) and the amount of crosslinking observed was unchanged in the presence of resveratrol, nicotinamide and curcumin; however, vanadate ions reduced the amount of crosslinked product observed (Fig. 1c).

For Peer Review

ScholarOne Support 1-434/964-4100

Steady state enzyme kinetics: no cooperativity with either NADH or NADPH

Lot6p can use both NADH and NADPH as electron donors; the $K_{m,app}$ for NADH was 273±35 μM and for NAD(P)H it was 131±22 μM. The $k_{cat,app}$ values for NADH and NADPH were 297±11 s^{-1} and 449±29 s^{-1} respectively (Fig. 2). Lot6p exhibits Michaelis-Menten kinetics (i.e. no detectable cooperativity) towards both electron donors with a Hill coefficient of 1.05±0.08 and 0.99±0.07 for NADH and NADPH respectively (Fig. 2).

Quinone oxidoreductase inhibitors stabilise Lot6p

The melting temperature of Lot6p, as judged by TSF, was 56.9±0.4 °C in HEPES buffer. Lot6p is slightly stabilised by phosphate ions; the T_m increased to 58.9±0.4 °C in 50 mM phosphate buffer (Supplementary Fig. S1). Resveratrol and nicotinamide stabilised Lot6p in a saturatable, concentration-dependent manner. The apparent dissociation constants with resveratrol and nicotinamide were 0.091±0.026 mM and 24.5±3.4 mM respectively (Fig. 3).

Inhibition of Lot6p is negatively cooperative with some compounds

The oxidoreductase activity of Lot6p was inhibited by curcumin, resveratrol, nicotinamide and vanadate. Dixon plots for all four compounds with NADH and NADPH as the reducing agent intersected as expected for competitive inhibition (Dixon, 1953). For each inhibitor except vanadate, the $K_{i,app}$ values obtained with NADH and NADPH were similar (Fig. 4; Table 1). Of the organic compounds, nicotinamide has the highest $K_{i,app}$ followed by curcumin and resveratrol which was the most effective inhibitor tested (Fig. 4; Table 1). Lot6p exhibits negative cooperativity with the inhibitors resveratrol, curcumin, and vanadate when inhibiting

ScholarOne Support 1-434/964-4100

For Peer Review

with respect to both NADH and NADPH; in contrast, nicotinamide does not induce negative cooperativity in Lot6p with either electron donor (Fig. 5; Table 2).

Molecular modelling of Lot6p and inhibitors

Nicotinamide, resveratrol and curcumin were all predicted to bind in the enzyme's active site, lying across the partly exposed surface of the isoalloxazine ring of the FMN cofactor, consistent with their role as competitive inhibitors (Fig. 6, left column). The two larger molecules, resveratrol and curcumin, extend beyond the active site into a cleft between the two polypeptide chains of the Lot6p dimer. Interestingly, resveratrol is predicted to make contact with an α-helix (residues Ser-130 to Leu-143) which links the two active sites of the dimeric enzyme (Fig. 6, right column). Curcumin contacts the equivalent α-helix in the other subunit. The smaller molecule, nicotinamide, does not contact this helix. Vanadate could, potentially, bind at a variety of sites including those for the three phosphate groups in NADPH. In the absence of any structures of quinone oxidoreductases bound to vanadate, no modelling was attempted with this inhibitor.

Mutation of a key residue reduces the degree of negative cooperativity

From the molecular models, we noticed that resveratrol contacts the α-helix which links the two active sites close to a glycine residue (Gly-142). Given the role of glycine in protein flexibility and the importance of such mobility in phenomena such as cooperativity (Goodey & Benkovic, 2008), we reasoned that altering this residue might affect cooperativity towards the inhibitors. Alteration of Gly-142 to serine results in an active enzyme, which is dimeric, has Michaelis-Menten kinetics with NADH and is inhibited by resveratrol and vanadate (Supplementary Fig S2, S3, S4;

For Peer Review

ScholarOne Support 1-434/964-4100

Table 3). The apparent inhibition constants for these compounds with respect to NADH were increased approximately two-fold (Table 3). The enzyme is slightly more stable towards thermal denaturation than the wild type (T_m values of 60.9±0.2 ºC and 61.5±0.6 ºC in phosphate and hepes buffer respectively; Supplementary Fig. S5). This is consistent with a less flexible overall structure. Resveratrol and nicotinamide both stabilise the G142S variant protein, with apparent dissociation constants similar to those of the wild-type (Table 3, Supplementary Fig. S6). However, the degree of negative cooperativity towards resveratrol and vanadate was less than that seen with the wild type; for both compounds, the Hill coefficient rose towards one (Table 3, Fig. 7).

Discussion

Previous studies of Lot6p have concentrated on its activity with NADPH as an electron donor (Sollner *et al.*, 2007). Here, it is demonstrated that NADH functions as an electron donor, albeit with a higher apparent Michaelis constant and lower turnover number. Lot6p's location in the cytoplasm (Sollner *et al.*, 2007) means that it is more likely to encounter NADPH since the NADPH:NADH concentration ratio in the cytoplasm is generally greater than one (Jacbonson & Kaplan, 1957). However, it has been demonstrated that, in *S. cerevisiae*, environmental changes (e.g. altered nutrient sources) can alter this ratio (Satrustegui *et al.*, 1983; Nissen *et al.*, 2001; Celton *et al.*, 2012; Ask *et al.*, 2013). Therefore, both reducing agents are likely to be important *in vivo*. Despite the dimeric nature of the enzyme, and the involvement of residues from both polypeptides in the two active sites, no cooperativity with respect to NADH or NADPH was detected in our experiments.

For Peer Review

ScholarOne Support 1-434/964-4100

Through thermal scanning fluorimetry experiments, we established that resveratrol, nicotinamide and vanadate ions all bind to, and stablise, Lot6p. Furthermore, these molecules (and curcumin) competitively inhibit the enzyme with respect to NAD(P)H – all except nicotinamide with negative cooperativity. Negative cooperativity towards inhibitors has previously been observed with mammalian NQO1 when inhibited with dicoumarol – although the molecular mechanism and physiological significance remains obscure (Rase *et al.*, 1976). The molecular models (Fig. 6) suggest a potential mechanism for inter-active site communication and also why nicotinamide is unable to initiate this. Both resveratrol and curcumin are predicted to contact an extended α-helix at the interface between the two polypeptides of the dimer. This helix links the two active sites and so it is plausible that alterations to its conformation induced by an inhibitor binding at one active site may affect the conformation of the second active site. Nicotinamide is predicted to bind parallel to the FMN cofactor and does not make contact with this helix; therefore it would be unable to initiate information transmission between the active sites. Given that, like all models, these should be treated with some caution, we tested the hypothesis by mutating a glycine residue in this helix. The resulting protein had similar kinetic properties and stability to the wild type protein, but showed less negative cooperativity (i.e. higher value of *h*) towards resveratrol and vanadate. This result supports the hypothesis that this helix plays a key role in transmitting information between the active sites in Lot6p. It also confirms that the non-Michaelian kinetics observed with inhibitors arises from genuine inter-active site cooperativity and not from intra-molecular aggregation or some other artefact.

For Peer Review

ScholarOne Support 1-434/964-4100

The physiological importance of the negative cooperativity observed in Lot6p is not yet clear. In many signalling systems, negative cooperativity functions to extend the concentration range over which the system is sensitive to concentration changes (Ferrell, 2009). Therefore it is possible that some, as yet unidentified, naturally occurring molecule in the yeast cytoplasm regulates Lot6p's activity and perhaps also its role in apoptosis or in the proteasome.

Acknowledgements

CFM thanks the Department of Employment and Learning (Northern Ireland) for a PhD studentship. We thank Profs Mario Bianchet and Mario Amzel (Johns Hopkins University Medical School, Baltimore, USA) for sharing the structure of human NQO1 bound to $NADP^+$, Dr Eva Hyde (The University of Birmingham, UK) for suggesting the use of nicotinamide as an inhibitor of quinone oxidoreductases and Prof Aaron Maule (Queen's University, Belfast, UK) for access to a qPCR machine.

For Peer Review

ScholarOne Support 1-434/964-4100

References

Adams MA & Jia Z (2006) Modulator of drug activity B from *Escherichia coli*: crystal structure of a prokaryotic homologue of DT-diaphorase. *J Mol Biol* **359**: 455-465.

Andrade SL, Patridge EV, Ferry JG & Einsle O (2007) Crystal structure of the NADH:quinone oxidoreductase WrbA from *Escherichia coli*. *J Bacteriol* **189**: 9101-9107.

Anlezark GM, Melton RG, Sherwood RF, Coles B, Friedlos F & Knox RJ (1992) The bioactivation of 5-(aziridin-1-yl)-2,4-dinitrobenzamide (CB1954) - I. Purification and properties of a nitroreductase enzyme from *Escherichia coli* - a potential enzyme for antibody-directed enzyme prodrug therapy (ADEPT). *Biochem Pharmacol* **44**: 2289-2295.

Anusevicius Z, Sarlauskas J & Cenas N (2002) Two-electron reduction of quinones by rat liver NAD(P)H:quinone oxidoreductase: quantitative structure-activity relationships. *Arch Biochem Biophys* **404**: 254-262.

Anwar A, Dehn D, Siegel D, Kepa JK, Tang LJ, Pietenpol JA & Ross D (2003) Interaction of human NAD(P)H:quinone oxidoreductase 1 (NQO1) with the tumor suppressor protein p53 in cells and cell-free systems. *J Biol Chem* **278**: 10368-10373.

Ask M, Bettiga M, Mapelli V & Olsson L (2013) The influence of HMF and furfural on redox-balance and energy-state of xylose-utilizing *Saccharomyces cerevisiae*. *Biotechnol Biofuels* **6**: 22-6834-6-22.

Bradford MM (1976) A rapid and sensitive method for the quantitation of microgram quantities of protein utilizing the principle of protein-dye binding. *Anal Biochem* **72**: 248-254.

For Peer Review

ScholarOne Support 1-434/964-4100

Buryanovskyy L, Fu Y, Boyd M, Ma Y, Hsieh TC, Wu JM & Zhang Z (2004) Crystal structure of quinone reductase 2 in complex with resveratrol. *Biochemistry* **43**: 11417-11426.

Caballero A, Lazaro JJ, Ramos JL & Esteve-Nunez A (2005) PnrA, a new nitroreductase-family enzyme in the TNT-degrading strain *Pseudomonas putida* JLR11. *Environ Microbiol* **7**: 1211-1219.

Carey J, Brynda J, Wolfova J, Grandori R, Gustavsson T, Ettrich R & Smatanova IK (2007) WrbA bridges bacterial flavodoxins and eukaryotic NAD(P)H:quinone oxidoreductases. *Protein Sci* **16**: 2301-2305.

Celton M, Sanchez I, Goelzer A, Fromion V, Camarasa C & Dequin S (2012) A comparative transcriptomic, fluxomic and metabolomic analysis of the response of *Saccharomyces cerevisiae* to increases in NADPH oxidation. *BMC Genomics* **13**: 317-2164-13-317.

Chignell CF, Bilski P, Reszka KJ, Motten AG, Sik RH & Dahl TA (1994) Spectral and photochemical properties of curcumin. *Photochem Photobiol* **59**: 295-302.

Choi JW, Lee J, Nishi K, Kim YS, Jung CH & Kim JS (2008) Crystal structure of a minimal nitroreductase, ydjA, from *Escherichia coli* K12 with and without FMN cofactor. *J Mol Biol* **377**: 258-267.

Dinkova-Kostova AT & Talalay P (2010) NAD(P)H:quinone acceptor oxidoreductase 1 (NQO1), a multifunctional antioxidant enzyme and exceptionally versatile cytoprotector. *Arch Biochem Biophys* **501**: 116-123.

Dixon M (1953) The determination of enzyme inhibitor constants. *Biochem J* **55**: 170-171.

Ferrell JE,Jr (2009) Q&A: Cooperativity. *J Biol* **8**: 53.

For Peer Review

ScholarOne Support 1-434/964-4100

Forneris F, Orru R, Bonivento D, Chiarelli LR & Mattevi A (2009) ThermoFAD, a Thermofluor-adapted flavin ad hoc detection system for protein folding and ligand binding. *FEBS J* **276**: 2833-2840.

Gong X, Gutala R & Jaiswal AK (2008) Quinone oxidoreductases and vitamin K metabolism. *Vitam Horm* **78**: 85-101.

Gong X, Kole L, Iskander K & Jaiswal AK (2007) NRH:quinone oxidoreductase 2 and NAD(P)H:quinone oxidoreductase 1 protect tumor suppressor p53 against 20s proteasomal degradation leading to stabilization and activation of p53. *Cancer Res* **67**: 5380-5388.

Goodey NM & Benkovic SJ (2008) Allosteric regulation and catalysis emerge via a common route. *Nat Chem Biol* **4**: 474-482.

Hill AV (1910) The possible effects of the aggregation of molecules of haemoglobin on its dissociation curve. *J Physiol (Lond)* **40**: 4-7.

Hong Y, Wang G & Maier RJ (2008) The NADPH quinone reductase MdaB confers oxidative stress resistance to *Helicobacter hepaticus*. *Microb Pathog* **44**: 169-174.

Hosoda S, Nakamura W & Hayashi K (1974) Properties and reaction mechanism of DT diaphorase from rat liver. *J Biol Chem* **249**: 6416-6423.

Ito K, Nakanishi M, Lee WC *et al.* (2006) Three-dimensional structure of AzoR from *Escherichia coli*. An oxidereductase conserved in microorganisms. *J Biol Chem* **281**: 20567-20576.

Jacbonson KB & Kaplan NO (1957) Pyridine coenzymes of subcellular tissue fractions. *J Biol Chem* **226**: 603-613.

Kobori T, Sasaki H, Lee WC, Zenno S, Saigo K, Murphy ME & Tanokura M (2001) Structure and site-directed mutagenesis of a flavoprotein from *Escherichia coli* that

For Peer Review

ScholarOne Support 1-434/964-4100

reduces nitrocompounds: alteration of pyridine nucleotide binding by a single amino acid substitution. *J Biol Chem* **276**: 2816-2823.

Krieger E, Joo K, Lee J *et al.* (2009) Improving physical realism, stereochemistry, and side-chain accuracy in homology modeling: Four approaches that performed well in CASP8. *Proteins* **77 Suppl 9**: 114-122.

Li R, Bianchet MA, Talalay P & Amzel LM (1995) The three-dimensional structure of NAD(P)H:quinone reductase, a flavoprotein involved in cancer chemoprotection and chemotherapy: mechanism of the two-electron reduction. *Proc Natl Acad Sci U S A* **92**: 8846-8850.

Liger D, Graille M, Zhou CZ *et al.* (2004) Crystal structure and functional characterization of yeast YLR011wp, an enzyme with NAD(P)H-FMN and ferric iron reductase activities. *J Biol Chem* **279**: 34890-34897.

LinWu SW, Wu CA, Peng FC & Wang AH (2012) Structure-based development of bacterial nitroreductase against nitrobenzodiazepine-induced hypnosis. *Biochem Pharmacol* **83**: 1690-1699.

Long DJ,2nd & Jaiswal AK (2000) NRH:quinone oxidoreductase2 (NQO2). *Chem Biol Interact* **129**: 99-112.

Lovering AL, Hyde EI, Searle PF & White SA (2001) The structure of *Escherichia coli* nitroreductase complexed with nicotinic acid: three crystal forms at 1.7 A, 1.8 A and 2.4 A resolution. *J Mol Biol* **309**: 203-213.

Marquardt D (1963) An algorithm for least squares estimation of nonlinear parameters. *SIAM J Appl Math* **11**: 431-441.

Mercier C, Chalansonnet V, Orenga S & Gilbert C (2013) Characteristics of major *Escherichia coli* reductases involved in aerobic nitro and azo reduction. *J Appl Microbiol* .

ScholarOne Support 1-434/964-4100

Miseviciene L, Anusevicius Z, Sarlauskas J & Cenas N (2006) Reduction of nitroaromatic compounds by NAD(P)H:quinone oxidoreductase (NQO1): the role of electron-accepting potency and structural parameters in the substrate specificity. *Acta Biochim Pol* **53**: 569-576.

Newsome JJ, Colucci MA, Hassani M, Beall HD & Moody CJ (2007) Benzimidazole- and benzothiazole-quinones: excellent substrates for NAD(P)H:quinone oxidoreductase 1. *Org Biomol Chem* **5**: 3665-3673.

Nissen TL, Anderlund M, Nielsen J, Villadsen J & Kielland-Brandt MC (2001) Expression of a cytoplasmic transhydrogenase in *Saccharomyces cerevisiae* results in formation of 2-oxoglutarate due to depletion of the NADPH pool. *Yeast* **18**: 19-32.

Nolan KA, Zhao H, Faulder PF *et al.* (2007) Coumarin-Based Inhibitors of Human NAD(P)H:Quinone Oxidoreductase-1. Identification, Structure-Activity, Off-Target Effects and In Vitro Human Pancreatic Cancer Toxicity. *J Med Chem* **50**: 6316-6325.

Onyenwoke RU & Wiegel J (2007) Iron (III) reduction: A novel activity of the human NAD(P)H:oxidoreductase. *Biochem Biophys Res Commun* **353**: 389-393.

Patridge EV & Ferry JG (2006) WrbA from *Escherichia coli* and *Archaeoglobus fulgidus* is an NAD(P)H:quinone oxidoreductase. *J Bacteriol* **188**: 3498-3506.

Prosser GA, Copp JN, Syddall SP *et al.* (2010) Discovery and evaluation of *Escherichia coli* nitroreductases that activate the anti-cancer prodrug CB1954. *Biochem Pharmacol* **79**: 678-687.

Rase B, Bartfai T & Ernster L (1976) Purification of DT-diaphorase by affinity chromatography. Occurrence of two subunits and nonlinear Dixon and Scatchard plots of the inhibition by anticoagulants. *Arch Biochem Biophys* **172**: 380-386.

Sarlauskas J, Dickancaite E, Nemeikaite A, Anusevicius Z, Nivinskas H, Segura-Aguilar J & Cenas N (1997) Nitrobenzimidazoles as substrates for DT-diaphorase and

For Peer Review

ScholarOne Support 1-434/964-4100

redox cycling compounds: their enzymatic reactions and cytotoxicity. *Arch Biochem Biophys* **346**: 219-229.

Satrustegui J, Bautista J & Machado A (1983) NADPH/$NADP^+$ ratio: regulatory implications in yeast glyoxylic acid cycle. *Mol Cell Biochem* **51**: 123-127.

Smith AL, Erwin AL, Kline T, Unrath WC, Nelson K, Weber A & Howald WN (2007) Chloramphenicol is a substrate for a novel nitroreductase pathway in *Haemophilus influenzae*. *Antimicrob Agents Chemother* **51**: 2820-2829.

Sollner S, Durchschlag M, Frohlich KU & Macheroux P (2009a) The redox-sensing quinone reductase Lot6p acts as an inducer of yeast apoptosis. *FEMS Yeast Res* **9**: 885-891.

Sollner S, Deller S, Macheroux P & Palfey BA (2009b) Mechanism of flavin reduction and oxidation in the redox-sensing quinone reductase Lot6p from Saccharomyces cerevisiae. *Biochemistry* **48**: 8636-8643.

Sollner S, Schober M, Wagner A *et al.* (2009c) Quinone reductase acts as a redox switch of the 20S yeast proteasome. *EMBO Rep* **10**: 65-70.

Sollner S, Nebauer R, Ehammer H *et al.* (2007) Lot6p from Saccharomyces cerevisiae is a FMN-dependent reductase with a potential role in quinone detoxification. *FEBS J* **274**: 1328-1339.

Tie JK, Jin DY, Straight DL & Stafford DW (2011) Functional study of the vitamin K cycle in mammalian cells. *Blood* **117**: 2967-2974.

Tsvetkov P, Asher G, Reiss V, Shaul Y, Sachs L & Lotem J (2005) Inhibition of NAD(P)H:quinone oxidoreductase 1 activity and induction of p53 degradation by the natural phenolic compound curcumin. *Proc Natl Acad Sci U S A* **102**: 5535-5540.

Vella F, Ferry G, Delagrange P & Boutin JA (2005) NRH:quinone reductase 2: an enzyme of surprises and mysteries. *Biochem Pharmacol* **71**: 1-12.

For Peer Review

ScholarOne Support 1-434/964-4100

Wang W & Malcolm BA (1999) Two-stage PCR protocol allowing introduction of multiple mutations, deletions and insertions using QuikChange Site-Directed Mutagenesis. *BioTechniques* **26**: 680-682.

Yanto Y, Hall M & Bommarius AS (2010) Nitroreductase from *Salmonella typhimurium*: characterization and catalytic activity. *Org Biomol Chem* **8**: 1826-1832.

Zenno S, Koike H, Tanokura M & Saigo K (1996a) Gene cloning, purification, and characterization of NfsB, a minor oxygen-insensitive nitroreductase from *Escherichia coli*, similar in biochemical properties to FRase I, the major flavin reductase in *Vibrio fischeri*. *J Biochem* **120**: 736-744.

Zenno S, Koike H, Kumar AN, Jayaraman R, Tanokura M & Saigo K (1996b) Biochemical characterization of NfsA, the *Escherichia coli* major nitroreductase exhibiting a high amino acid sequence homology to Frp, a *Vibrio harveyi* flavin oxidoreductase. *J Bacteriol* **178**: 4508-4514.

Zhang L, Ohta A, Horiuchi H, Takagi M & Imai R (2001) Multiple mechanisms regulate expression of low temperature responsive (*LOT*) genes in Saccharomyces cerevisiae. *Biochem Biophys Res Commun* **283**: 531-535.

For Peer Review

ScholarOne Support 1-434/964-4100

Figure legends

Figure 1: **Expression and dimerization of recombinant Lot6p**. (A) SDS-PAGE (10%) showing the progress of a typical expression and purification of Lot6p. (B) Crosslinking of recombinant Lot6p with EDC (0, 4, 8, 16, 32, 64 mM) and BS^3 (0, 50, 100, 200, 400, 800 µM). The effects of solvent (DMSO 1 %(v/v)) and ligands (resveratrol 0.7 mM, curcumin 40 µM, nicotinamide 160 mM, vanadate 18 mM) on crosslinking by EDC (32 mM) and BS^3 (800 µM). In (A), (B) and (C) lane M represents the molecular mass markers (with masses shown to the left of the gel in kDa).

Figure 2: **Lot6p kinetics with electron donors.** Initial rates of DCPIP (70 µM) reduction were measured and plotted as a function of either NADH or NADPH concentration (top graphs). These data were replotted as linear Hill plots (bottom graphs). Each point represents the mean of three independent determinations and the error bars the standard error of these means.

Figure 3: **Ligands stabilise Lot6p against thermal denaturation.** Increasing concentrations of resveratrol and nicotinamide were mixed with Lot6p (0.25 µM) in Hepes-OH buffer (pH 7.3) and the melting temperature determined by TSF. The first derivative curves of the fluorescence against temperature (top) were used to determine T_m values, which were plotted against ligand concentration (bottom). Each point represents the mean of three values and error bars the standard errors of these means.

Figure 4: **Ligands inhibit the oxidoreductase activity of Lot6p.** Initial rates of DCPIP reduction were measured at different NADH (left column) and NADPH (right)

ScholarOne Support 1-434/964-4100

For Peer Review

concentrations in the presence of increasing concentrations of ligand. See Materials and Methods for the conditions of these experiments. Dixon plots (1/v against [Inhibitor]) were constructed and the $K_{i,app}$ estimated for each inhibitor. Each point represents the mean of three separate determinations and the error bars the standard errors of these means.

Figure 5: **Some inhibitors exhibit negative cooperativity**. Linear Hill plots with (A) NADH and (B) NADPH as the reducing agent were constructed in order to determine the Hill coefficient, *h*. See Materials and Methods for the conditions of these experiments. Each point represents the mean of three separate determinations and the error bars the standard errors of these means.

Figure 6: **Molecular modelling predicts how the inhibitors bind to Lot6p**. In the left hand column a close up of the active site with inhibitor bound is shown. In the right hand column the inhibitor is shown bound to one active site and, in the case of curcumin and resveratrol, contacting an α-helix (orange) which connects the two active sites of the enzyme. (Note that curcumin and resveratrol contact the equivalent helix in different subunits.) FMN is shown in yellow.

Figure 7: **The G142S variant of Lot6p has reduced negative cooperativity towards some inhibitors.** Linear Hill plots showing the effect of resveratrol and vanadate on the NADH mediated reduction of DCPIP. See Materials and Methods for the conditions of these experiments. Each point represents the mean of three separate determinations and the error bars the standard errors of these means.

For Peer Review

ScholarOne Support 1-434/964-4100

Tables

Table 1:

Inhibition of Lot6p.

Inhibitor	$K_{i,app}$/mM	
	with NADH	with NADPH
Resveratrol	0.067±0.003	0.063±0.033
Curcumin	5.8±1.0	5.0±2.5
Nicotinamide	20.0±4.8	11.9±4.5
Vanadate	21.1±4.3	3.4±0.2

Values are the mean of the intersection points in the Dixon plot and the errors are the standard deviation of these means.

For Peer Review

ScholarOne Support 1-434/964-4100

Table 2:

Hill coefficients (h) for the inhibition of Lot6p.

Inhibitor	Hill coefficient (h)	
	with NADH	with NADPH
Resveratrol	0.75±0.11	0.83 ±0.05
Curcumin	0.60±0.09	0.61 ±0.10
Nicotinamide	1.02±0.07	1.03 ±0.05
Vanadate	0.44±0.05	0.71 ±0.01

Values were determined by constructing three separate linearised Hill plots, each based on triplicate data. The values quoted are the means of the three estimates of h and the errors the standard deviations of these means.

For Peer Review

ScholarOne Support 1-434/964-4100

Table 3

Properties of the G142S variant of Lot6p

Property	Value
$K_{m,app}$ (NADH)	1200±110 μM
$k_{cat,,app}$ (NADH)	160+5 s^{-1}
h (NADH)	1.08±0.03
$K_{i,app}$ (Resveratrol)	0.059±0.030 mM
$K_{i,app}$ (Vanadate)	46±16 mM
$K_{D,app}$ (Resveratrol)	0.22±0.07 mM
$K_{D,app}$ (Nicotinamide)	20.8±2.3 mM
h (Resveratrol)	0.94±0.04
h (Vanadate)	0.82±0.08

For Peer Review

ScholarOne Support 1-434/964-4100

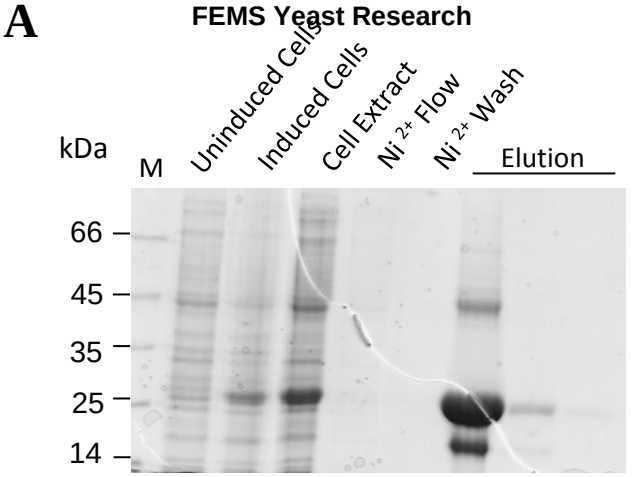
A
kDa
M
Uninduced Cells
Induced Cells
Cell Extract
Ni 2+ Flow
Ni 2+ Wash
Elution
66
45
35
25
14

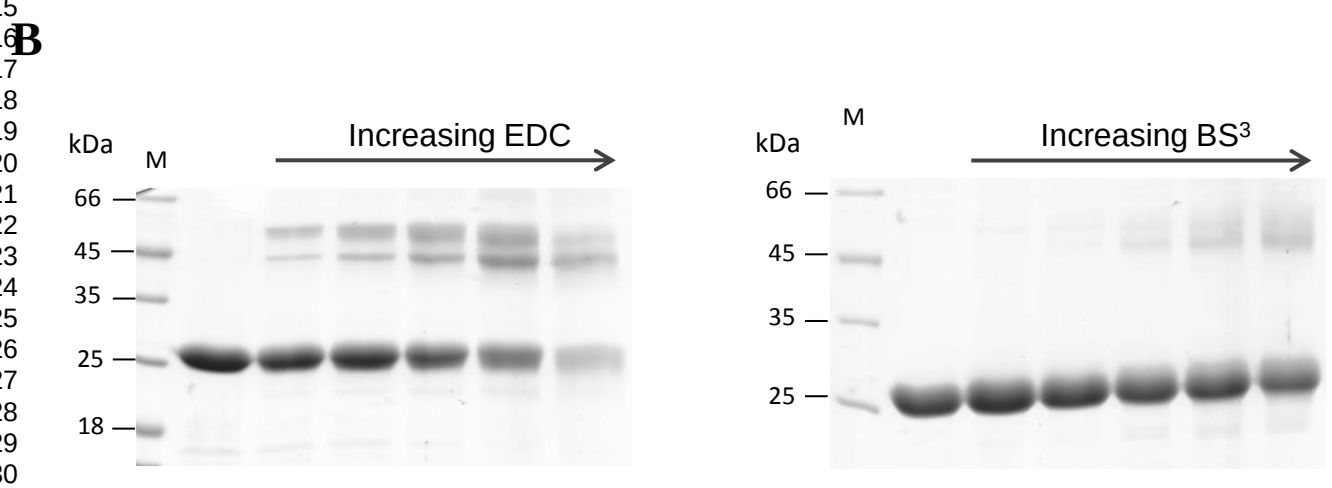
B
kDa
M
Increasing EDC
66
45
35
25
18
kDa
M
Increasing BS3
66
45
35
25

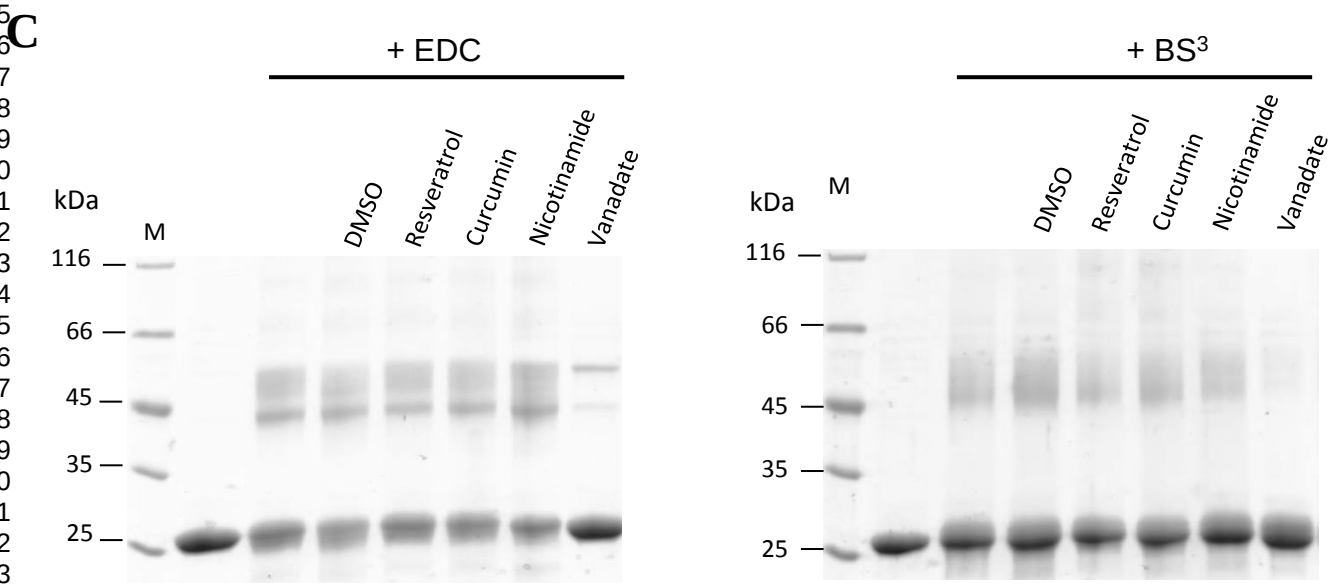
C
+ EDC
kDa
M
DMSO
Resveratrol
Curcumin
Nicotinamide
Vanadate
116
66
45
35
25
+ BS3
kDa
M
DMSO
Resveratrol
Curcumin
Nicotinamide
Vanadate
116
66
45
35
25

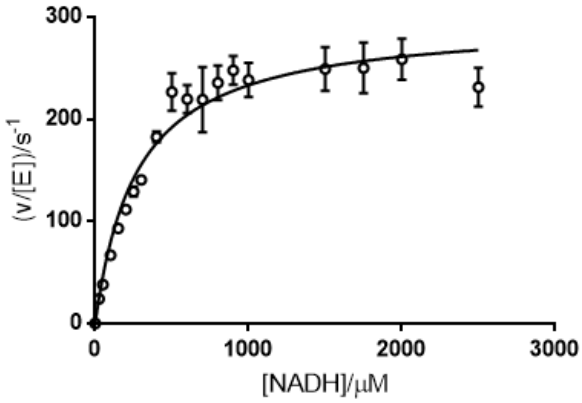
300
200
100
0
(v/[E])/s-1
0
1000
2000
3000
[NADH]/μM

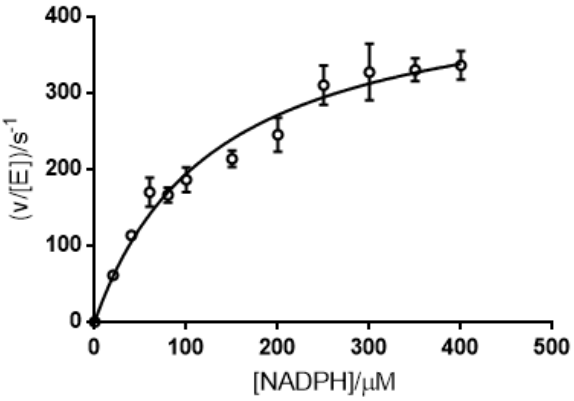
400
300
200
100
0
(v/[E])/s-1
0
100
200
300
400
500
[NADPH]/μM

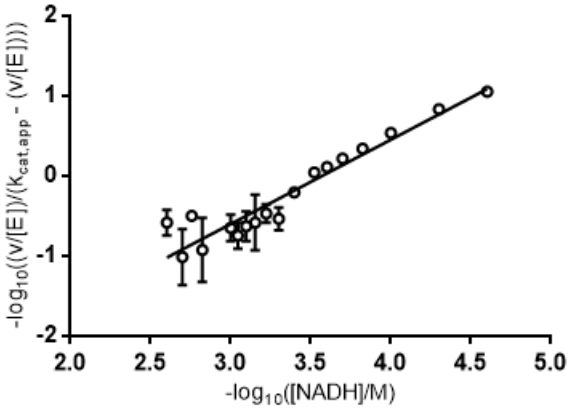
2
1
0
-1
-2
-log10((v/[E])/(Kcat,app - (v/[E])))
2.0
2.5
3.0
3.5
4.0
4.5
5.0
-log10([NADH]/M)

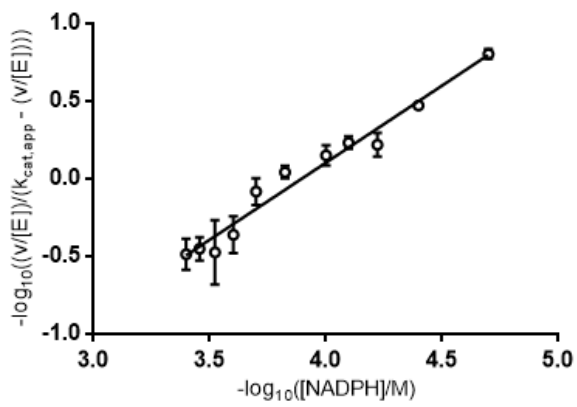
1.0
0.5
0.0
-0.5
-1.0
-log10((v/[E])/(Kcat,app - (v/[E])))
3.0
3.5
4.0
4.5
5.0
-log10([NADPH]/M)

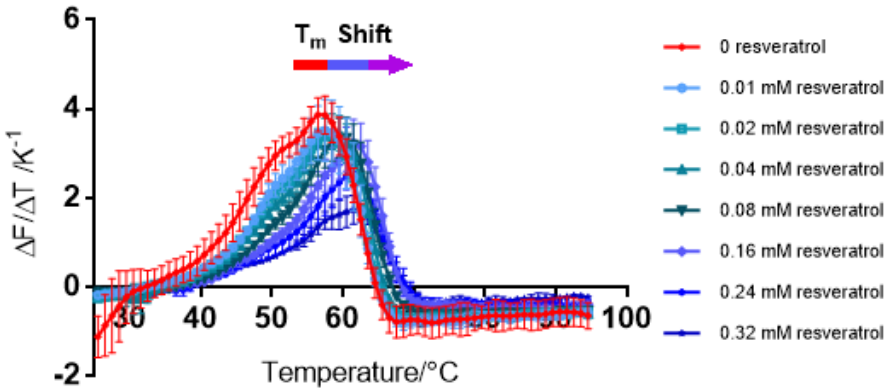
T_m Shift
ΔF/ΔT /K^-1
Temperature/°C
0 resveratrol
0.01 mM resveratrol
0.02 mM resveratrol
0.04 mM resveratrol
0.08 mM resveratrol
0.16 mM resveratrol
0.24 mM resveratrol
0.32 mM resveratrol

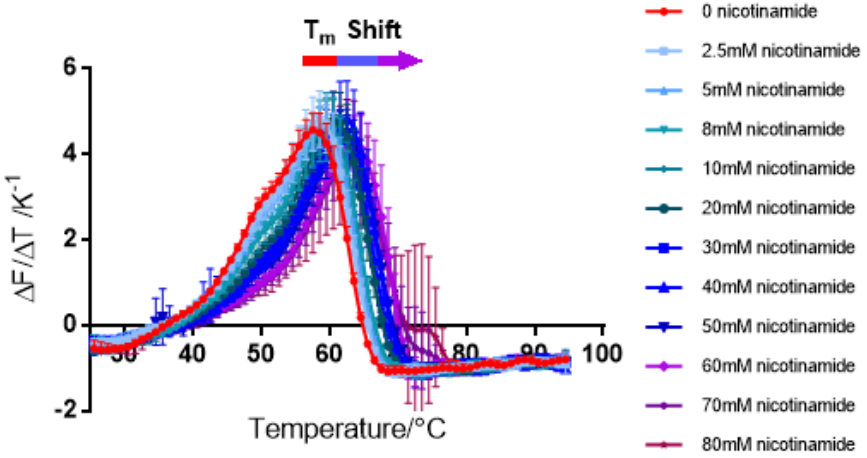
T_m Shift
ΔF/ΔT /K^-1
Temperature/°C
0 nicotinamide
2.5mM nicotinamide
5mM nicotinamide
8mM nicotinamide
10mM nicotinamide
20mM nicotinamide
30mM nicotinamide
40mM nicotinamide
50mM nicotinamide
60mM nicotinamide
70mM nicotinamide
80mM nicotinamide

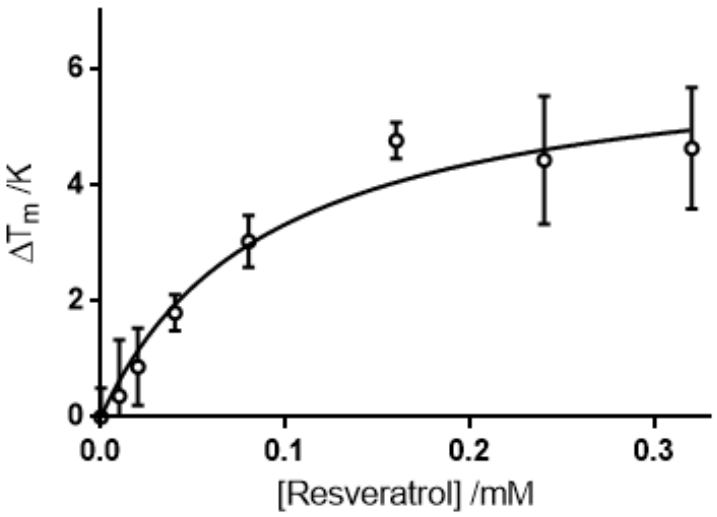
ΔT_m /K
[Resveratrol] /mM

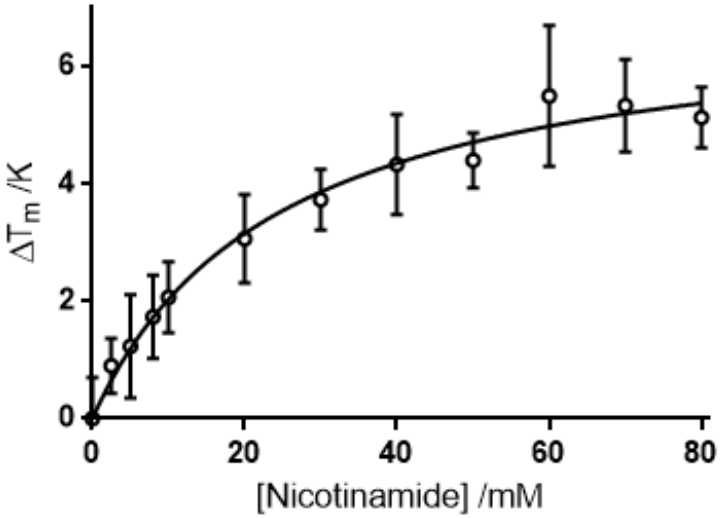
ΔT_m /K
[Nicotinamide] /mM

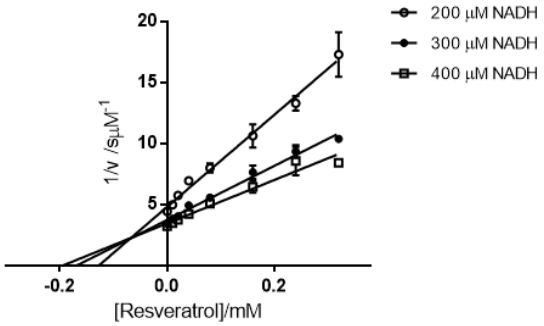
200 μM NADH
300 μM NADH
400 μM NADH
1/v /sμM-1
[Resveratrol]/mM

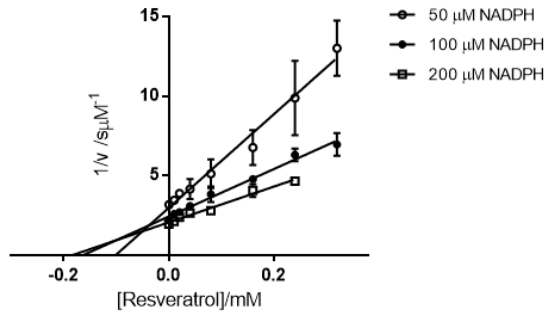
50 μM NADPH
100 μM NADPH
200 μM NADPH
1/v /sμM-1
[Resveratrol]/mM

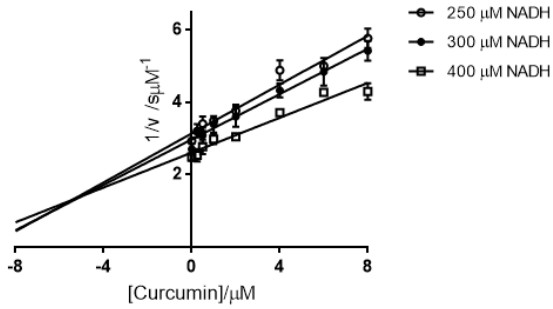
250 μM NADH
300 μM NADH
400 μM NADH
1/v /sμM-1
[Curcumin]/μM

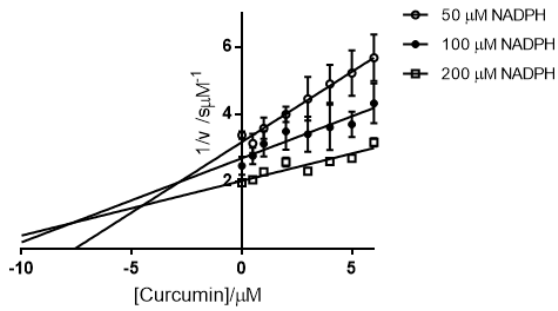
50 μM NADPH
100 μM NADPH
200 μM NADPH
1/v /sμM-1
[Curcumin]/μM

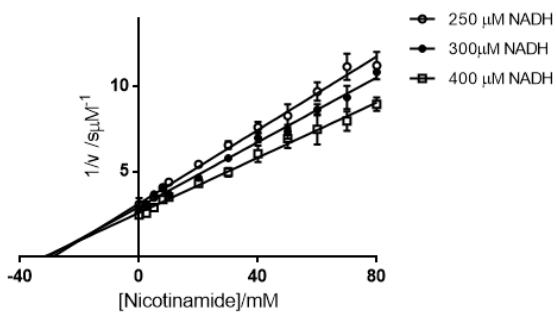
250 μM NADH
300μM NADH
400 μM NADH
1/v /sμM-1
[Nicotinamide]/mM

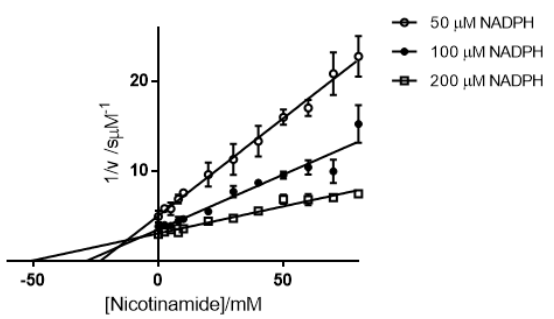
50 μM NADPH
100 μM NADPH
200 μM NADPH
1/v /sμM-1
[Nicotinamide]/mM

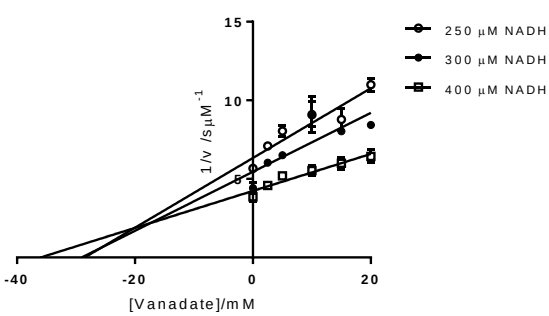
250 μM NADH
300 μM NADH
400 μM NADH
1/v /sμM-1
[Vanadate]/mM

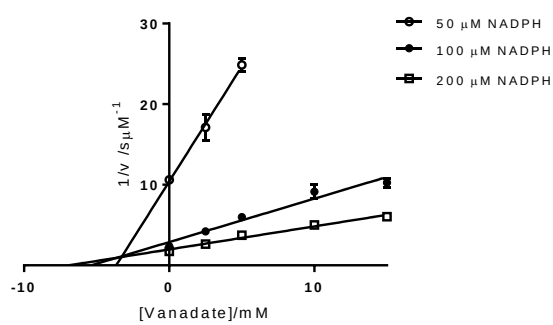
50 μM NADPH
100 μM NADPH
200 μM NADPH
1/v /sμM-1
[Vanadate]/mM

A

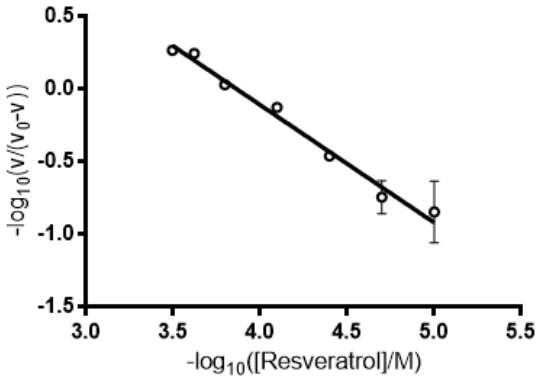

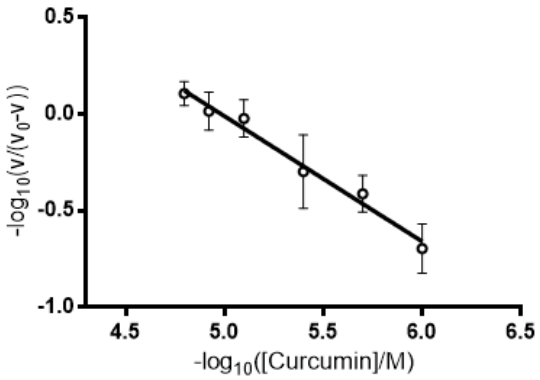

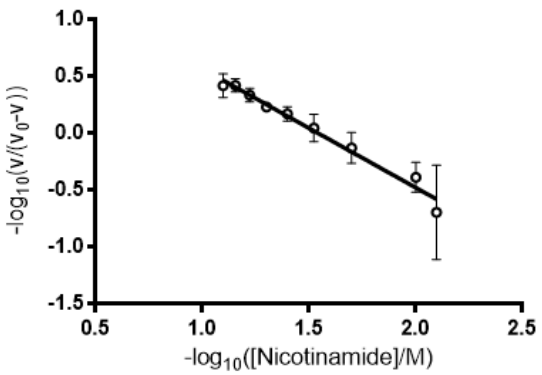

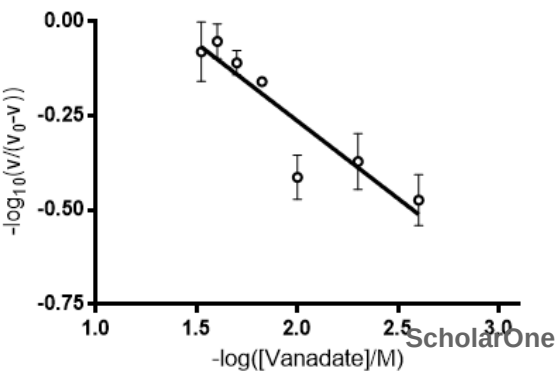

B

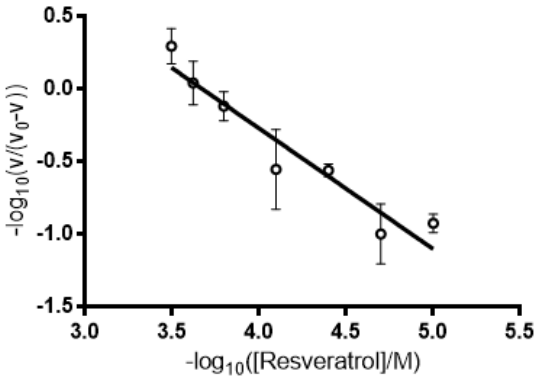

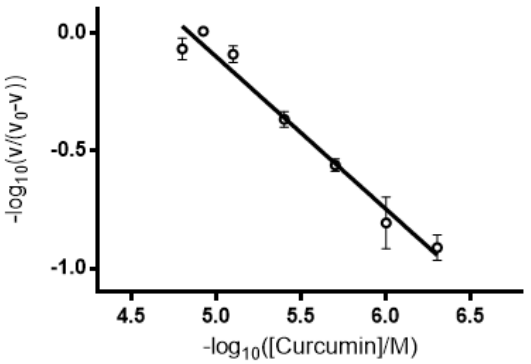

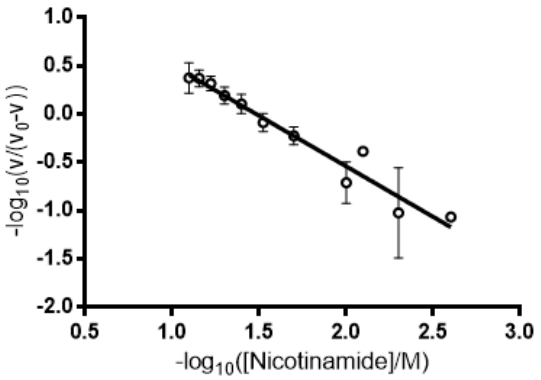

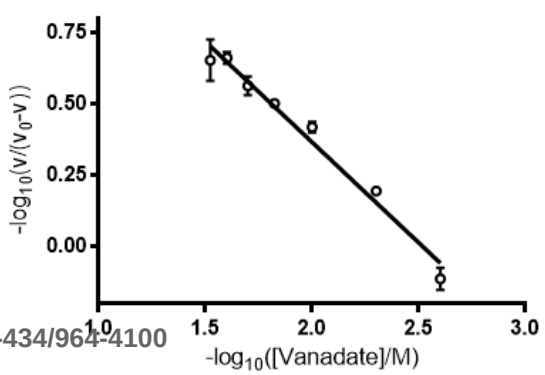

ScholarOne Support 1-434/964-4100

Curcumin

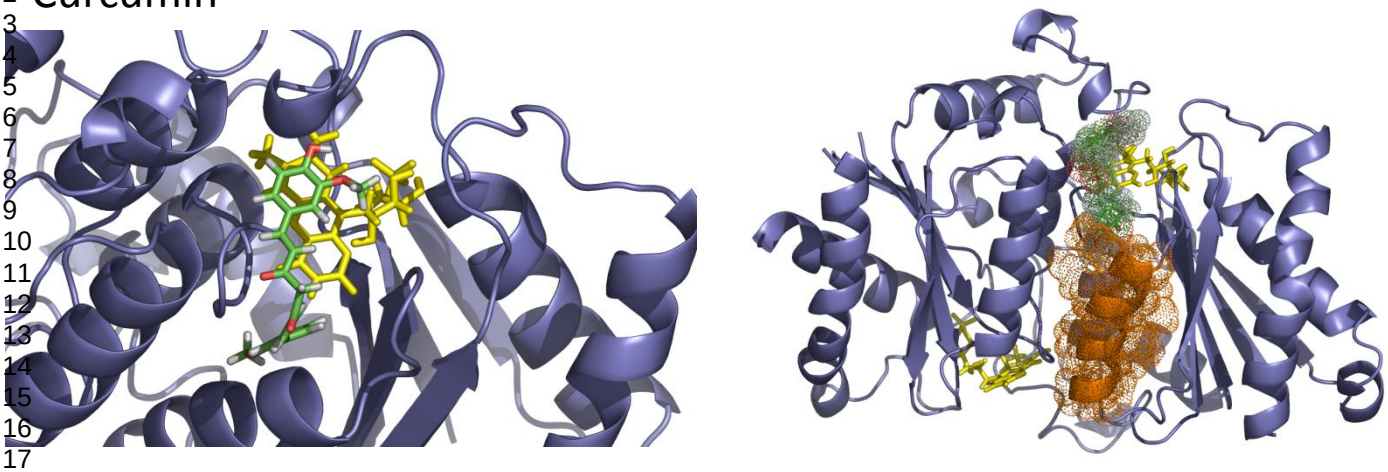

Resveratrol

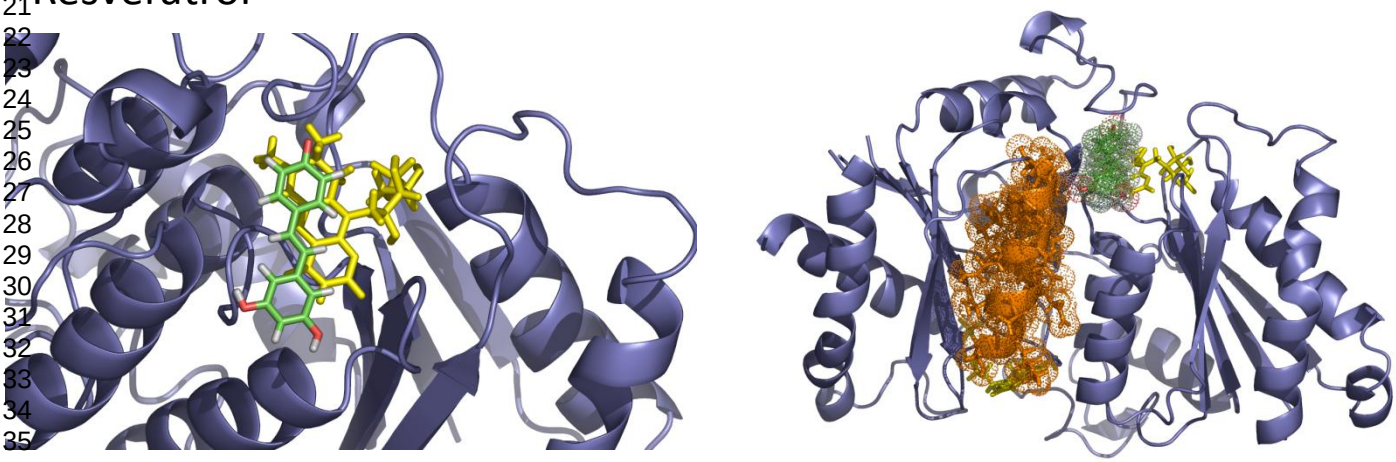

Nicotinamide

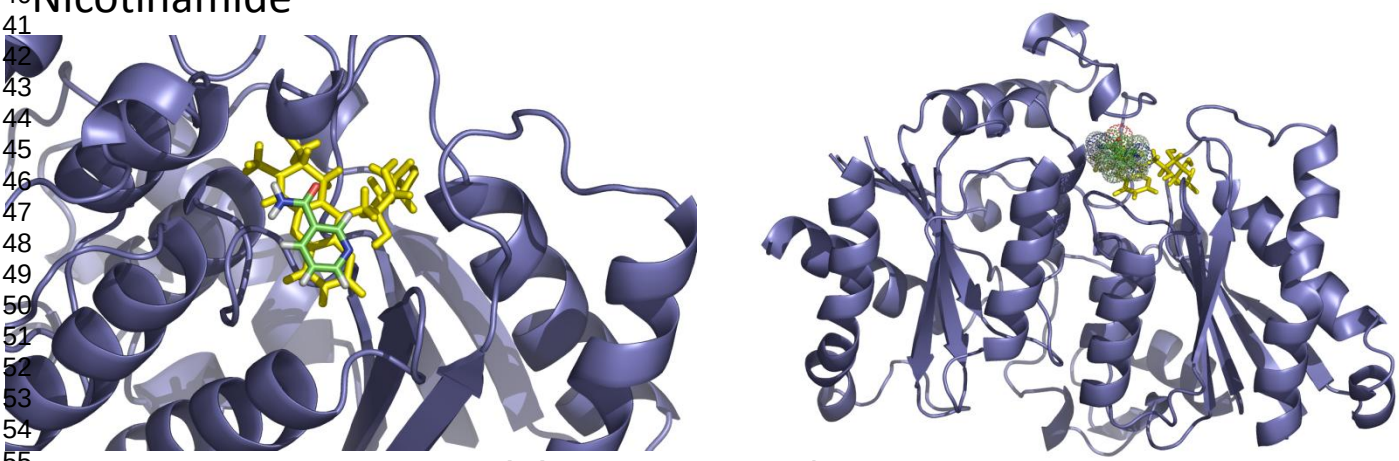

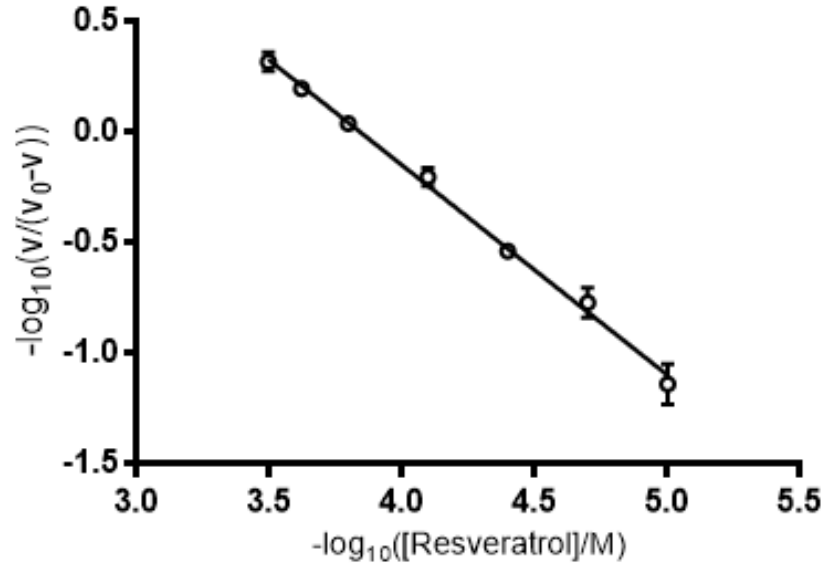
0.5
0.0
-0.5
-1.0
-1.5
3.0
3.5
4.0
4.5
5.0
5.5
-log10(v/(v0-v))
-log10([Resveratrol]/M)

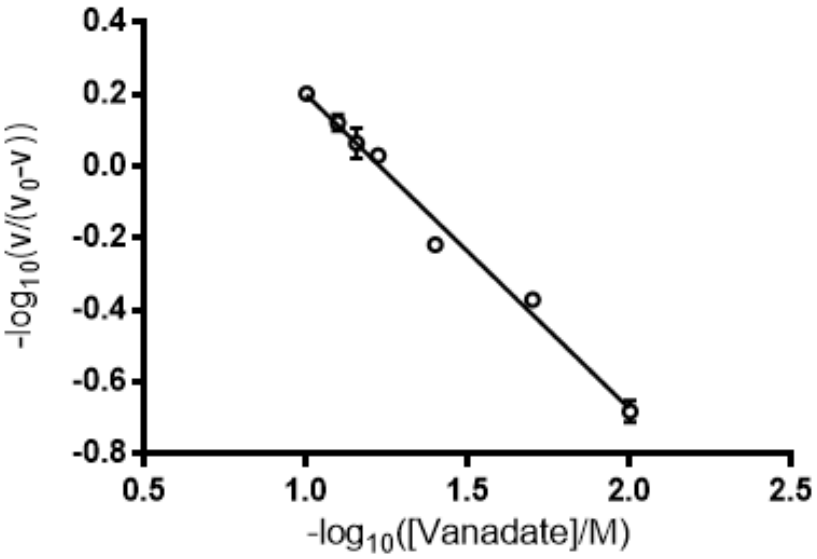
0.4
0.2
0.0
-0.2
-0.4
-0.6
-0.8
0.5
1.0
1.5
2.0
2.5
-log10(v/(v0-v))
-log10([Vanadate]/M)

Supplementary Figure S1: **Phosphate ions slightly stabilise Lot6p**. Melting point determination of Lot6p (0.25 μM) by TSF in Hepes-OH (pH 7.3) and phosphate buffer (pH 7.4).

Supplementary Figure S2: **The G142S variant of Lot6p forms dimers.** Upper panels: Crosslinking of the G142S variant with EDC (0, 4, 8, 16, 32, 64 mM) and BS^3 (0, 50, 100, 200, 400, 800 μM). Lower panels: The effects of solvent (DMSO 1 %(v/v)) and ligands (resveratrol 0.7 mM, curcumin 40 μM, nicotinamide 160 mM, vanadate 18 mM) on crosslinking by EDC (32 mM) and BS^3 (800 μM). In all gels, lane M represents the molecular mass markers (with masses shown to the left of the gel in kDa).

Supplementary Figure S3: **The G142S variant of Lot6p has Michaelis-Menten kinetics.** Initial rates of DCPIP (70 μM) reduction were measured and plotted as a function of NADH (upper panels). The data were replotted as a linear Hill plot (lower panels). Each point represents the mean of three independent determinations and the error bars the standard error of these means.

Supplementary Figure S4: **The G142S variant of Lot6p is inhibited by resveratrol and vanadate.** Initial rates of DCPIP reduction were measured at different NADH concentrations in the presence of increasing concentrations of inhibitor. See Materials and Methods for the conditions of these experiments. Dixon plots ($1/v$ against [Inhibitor]) were constructed and the $K_{i,app}$ estimated for each inhibitor. Each point represents the mean of three separate determinations and the error bars the standard errors of these means.

For Peer Review

Supplementary Figure S5: **The G142S variant of Lot6p has similar thermal stability to the wild type.** Melting point determination of G142S (0.25 μM) by TSF in Hepes-OH (pH 7.3) and phosphate buffer (pH 7.4).

Supplementary Figure S6: **The G142S variant of Lot6p is stabilised by resveratrol and nicotinamide.** Increasing concentrations of resveratrol and nicotinamide were mixed with G142S (0.25 μM) in Hepes-OH buffer (pH 7.3) and the melting temperature determined by TSF. The first derivative curves of the fluorescence against temperature were used to determine T_m values, which were plotted against ligand concentration. Each point represents the mean of three values and error bars the standard errors of these means.

For Peer Review

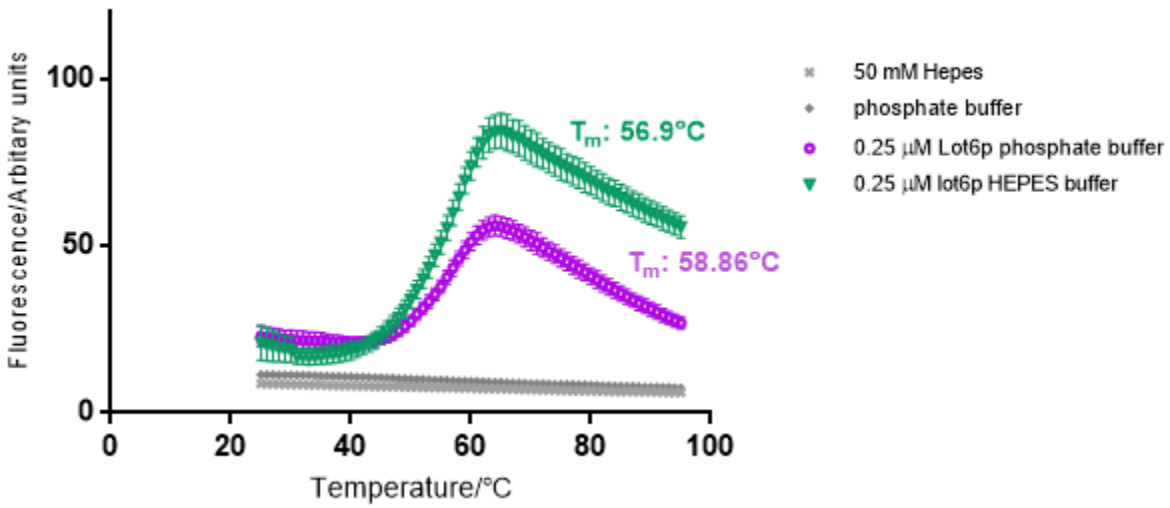
Fluorescence/Arbitary units
100
50
0
0
20
40
60
80
100
Temperature/°C
T_m: 56.9°C
T_m: 58.86°C
50 mM Hepes
phosphate buffer
0.25 µM Lot6p phosphate buffer
0.25 µM lot6p HEPES buffer

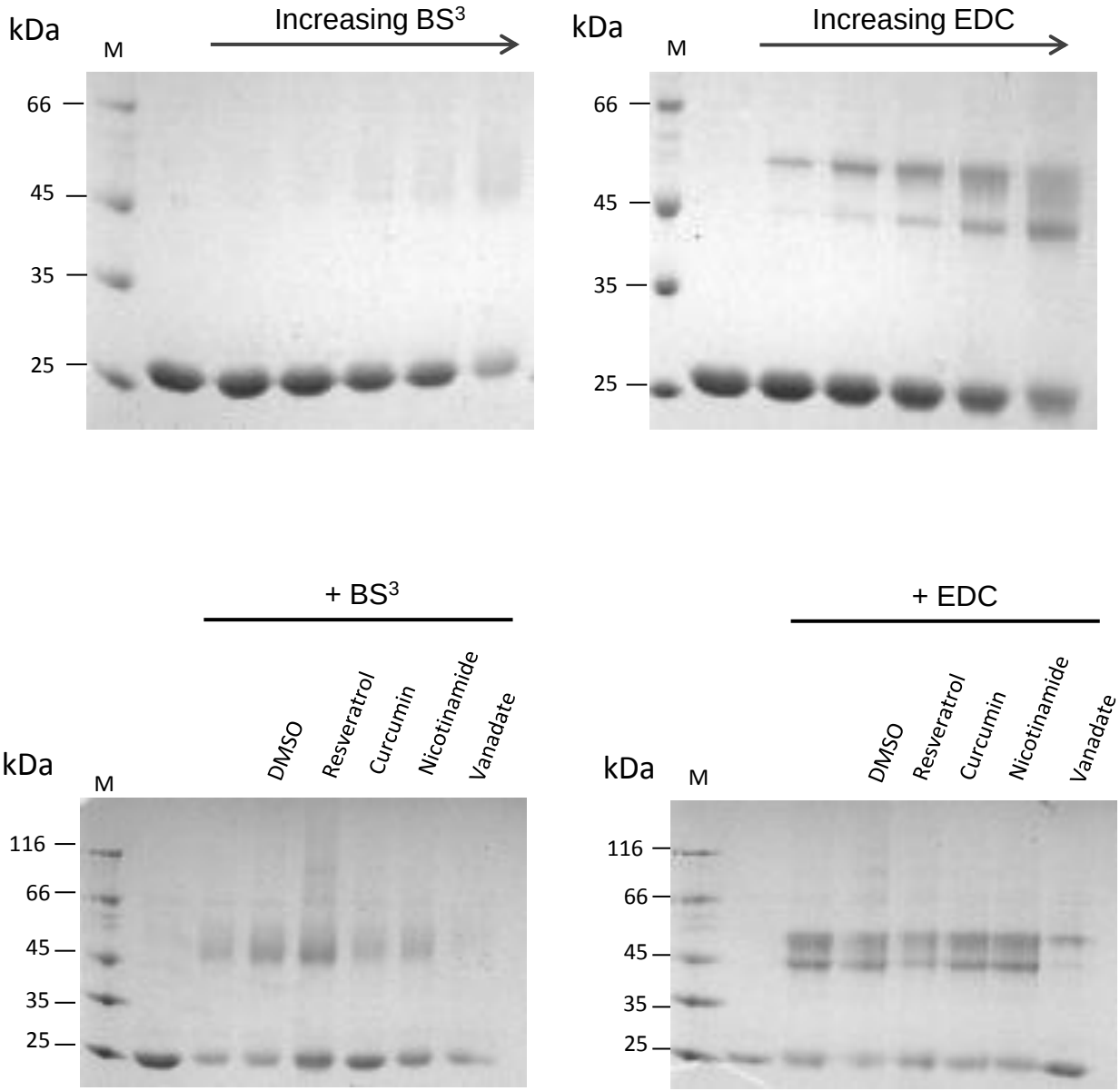
kDa
M
Increasing BS3
66
45
35
25
kDa
M
Increasing EDC
66
45
35
25
+ BS3
DMSO
Resveratrol
Curcumin
Nicotinamide
Vanadate
kDa
M
116
66
45
35
25
+ EDC
DMSO
Resveratrol
Curcumin
Nicotinamide
Vanadate
kDa
M
116
66
45
35
25

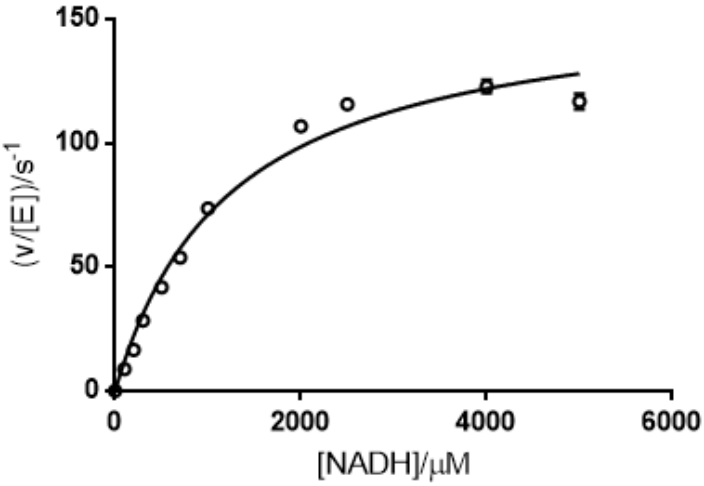
150
100
50
0
(v/[E])/s-1
0
2000
4000
6000
[NADH]/μM

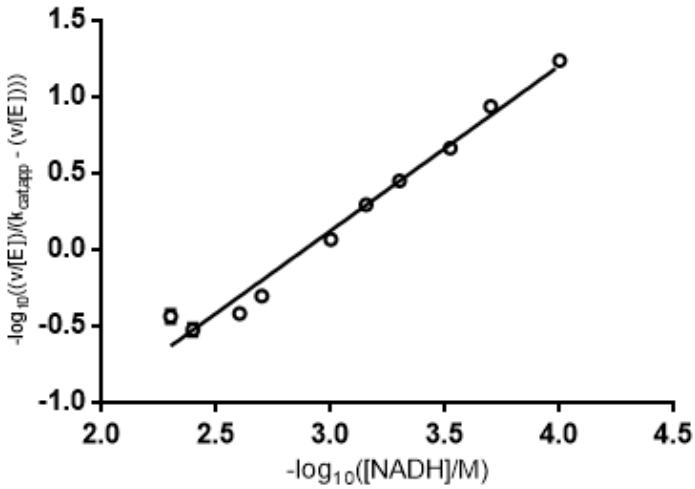
1.5
1.0
0.5
0.0
-0.5
-1.0
-log10((v/[E])/(kcatapp - (v/[E])))
2.0
2.5
3.0
3.5
4.0
4.5
-log10([NADH]/M)

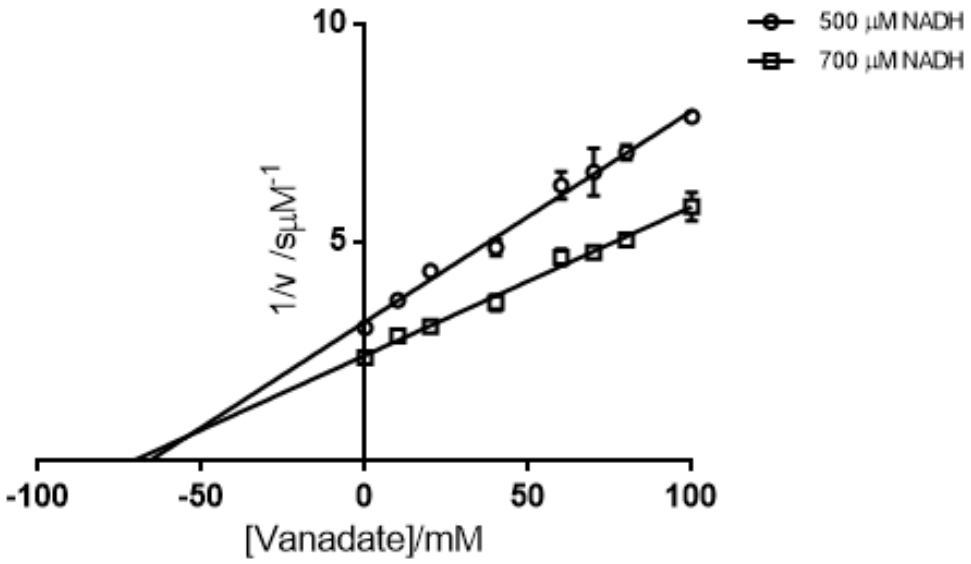
500 μM NADH
700 μM NADH
10
5
1/v /sμM-1
-100
-50
0
50
100
[Vanadate]/mM

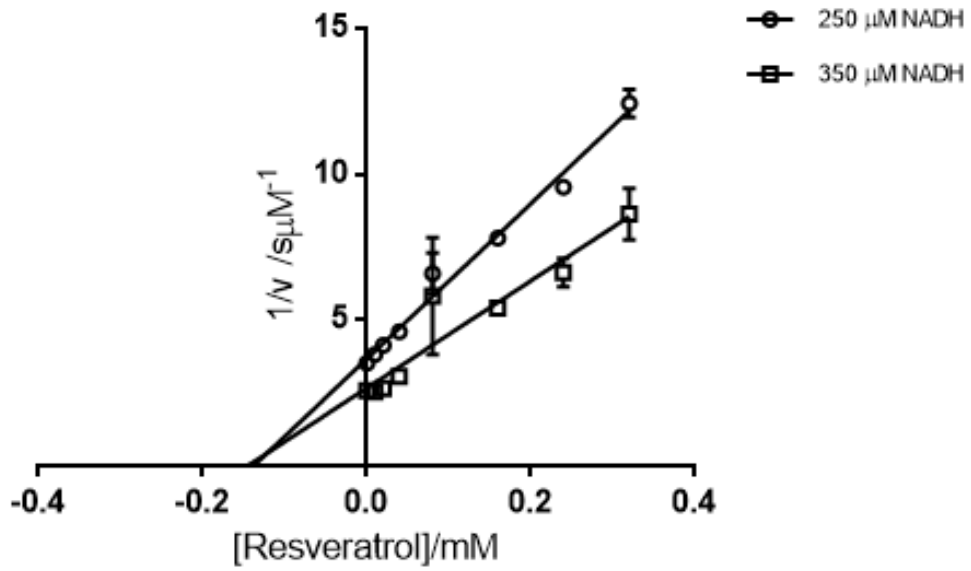
250 μM NADH
350 μM NADH
15
10
5
1/v /sμM-1
-0.4
-0.2
0.0
0.2
0.4
[Resveratrol]/mM

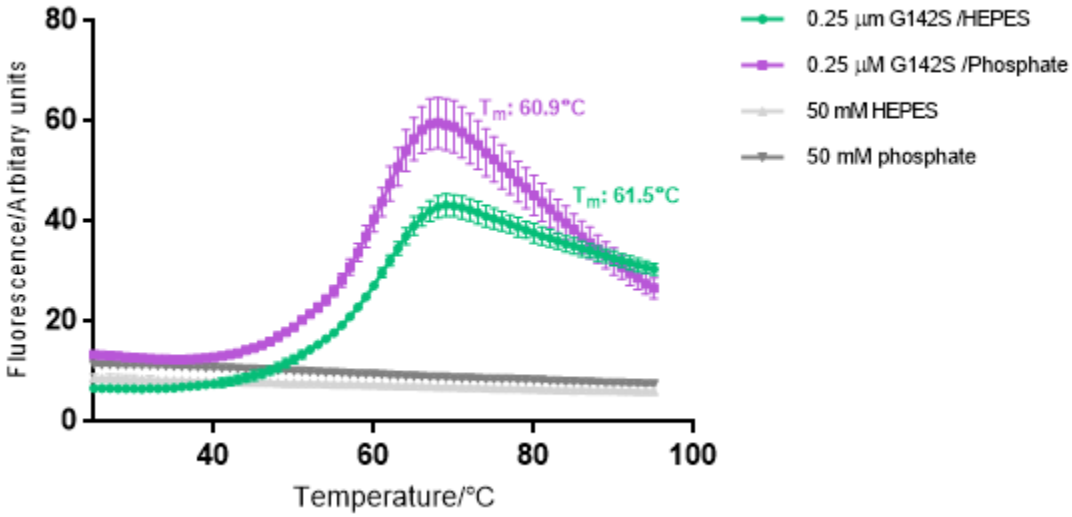
80
60
40
20
0
Fluorescence/Arbitary units
40
60
80
100
Temperature/°C
T_m: 60.9°C
T_m: 61.5°C
0.25 µm G142S /HEPES
0.25 µM G142S /Phosphate
50 mM HEPES
50 mM phosphate

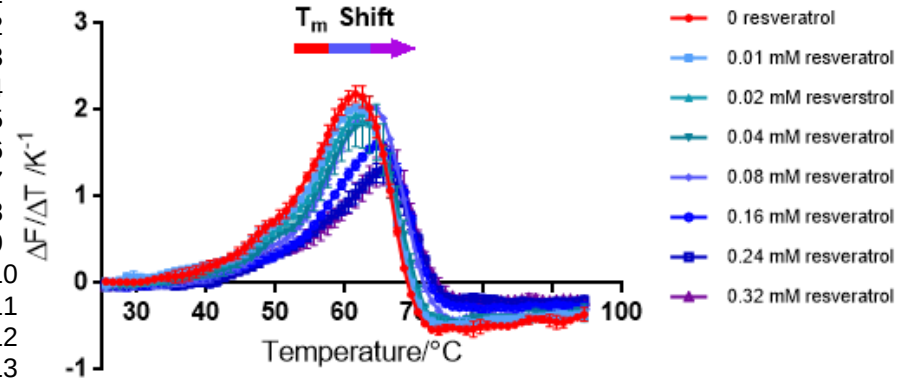
T_m Shift
$\Delta F/\Delta T$ /K^{-1}
Temperature/°C
0 resveratrol
0.01 mM resveratrol
0.02 mM resverstrol
0.04 mM resveratrol
0.08 mM resveratrol
0.16 mM resveratrol
0.24 mM resveratrol
0.32 mM resveratrol

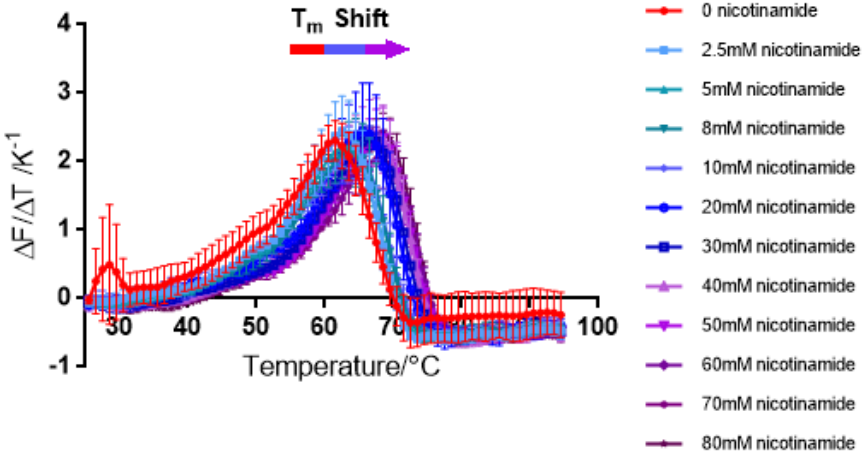
T_m Shift
$\Delta F/\Delta T$ /K^{-1}
Temperature/°C
0 nicotinamide
2.5mM nicotinamide
5mM nicotinamide
8mM nicotinamide
10mM nicotinamide
20mM nicotinamide
30mM nicotinamide
40mM nicotinamide
50mM nicotinamide
60mM nicotinamide
70mM nicotinamide
80mM nicotinamide

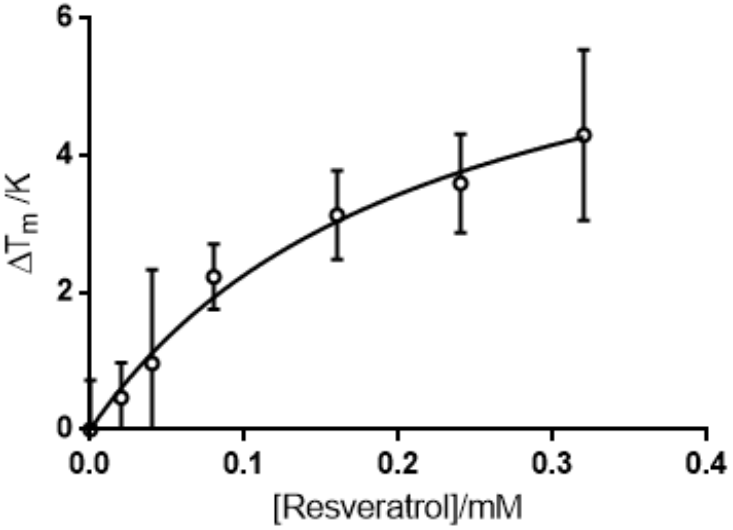
ΔT_m /K
[Resveratrol]/mM

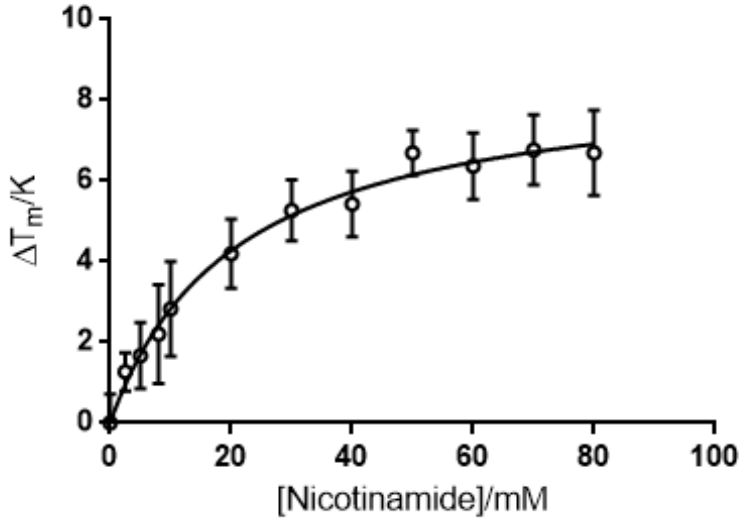
ΔT_m/K
[Nicotinamide]/mM